Nuclear structure studies through in-flight measurements

- Introduction
- Methods
- Physics Cases
- Perspectives

Peter Reiter
IKP, University of Cologne

Advances in Nuclear Physics
Goa, 9-18 November 2011

Nuclear structure studies through in-flight measurements

today

- Introduction
- Method: Coulomb excitation
at relativistic energies part I
- 1. Physics case: ‚Island of Inversion'
- Method: Coulomb excitation
at safe energies with instable ion beams

The role of γ-ray spectroscopy

Several approaches for in-beam γ-ray spectroscopy of bound states with fast exotic ion beams:

- Relativistic Projectile Coulomb excitation

- Inelastic proton scattering in inverse kinematics

- Nucleon removal reactions
  - direct one-nucleon removal
  - direct two-nucleon removal

- Single-step and two-step fragmentation reactions

In-beam γ-ray spectroscopy with reaccelerated exotic ion beams:

- Projectile Coulomb excitation below the barrier

Intermediate-energy Coulomb excitation

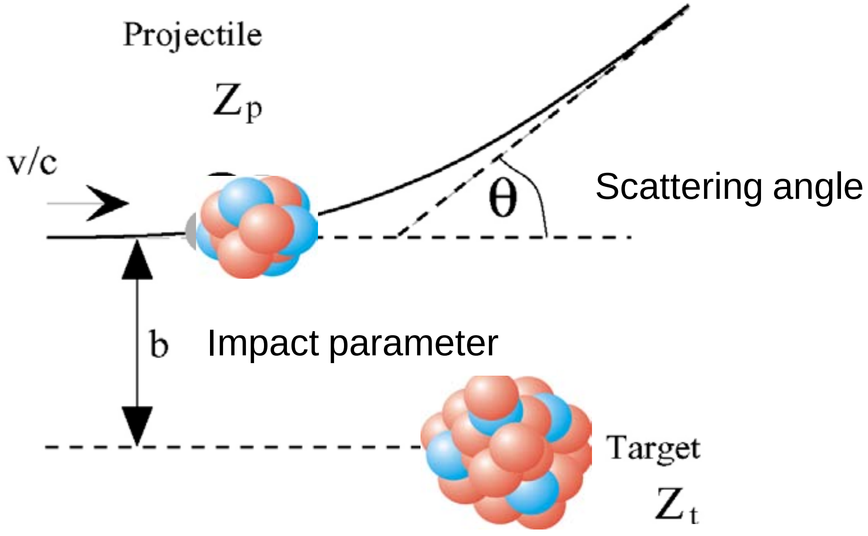

- σ_{Coul} = 87 mb
- B(E2↑) = 454(78) e^2fm^4
- $|\beta_2|$ = 0.49(4)
- Large transition matrix element indicates breakdown of N=20 shell gap

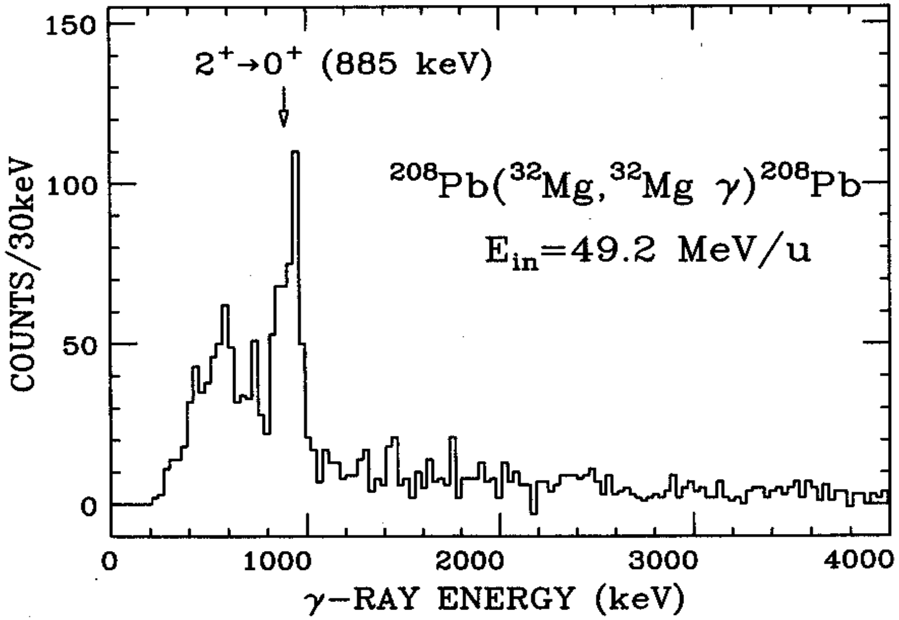

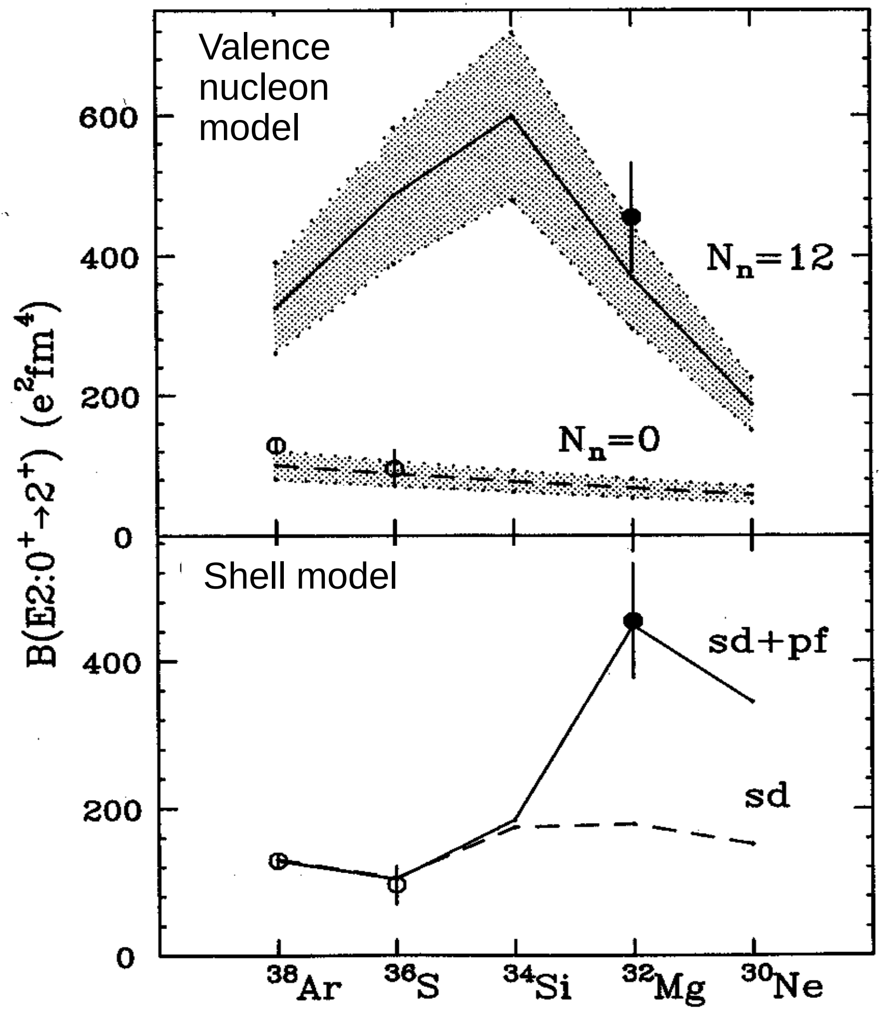

T. Motobayashi, *et al.*, Phys. Lett. B 346 (1995) 9

Inelastic proton scattering in inverse kinematics

Normal kinematics

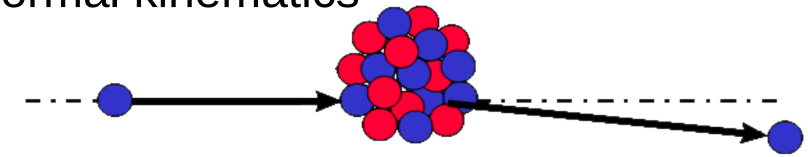

Inverse kinematics

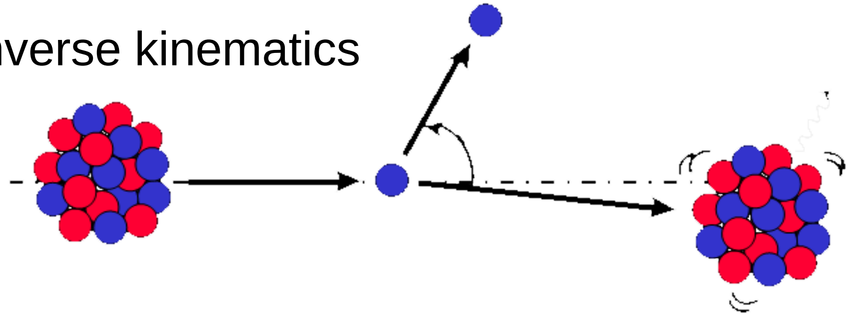

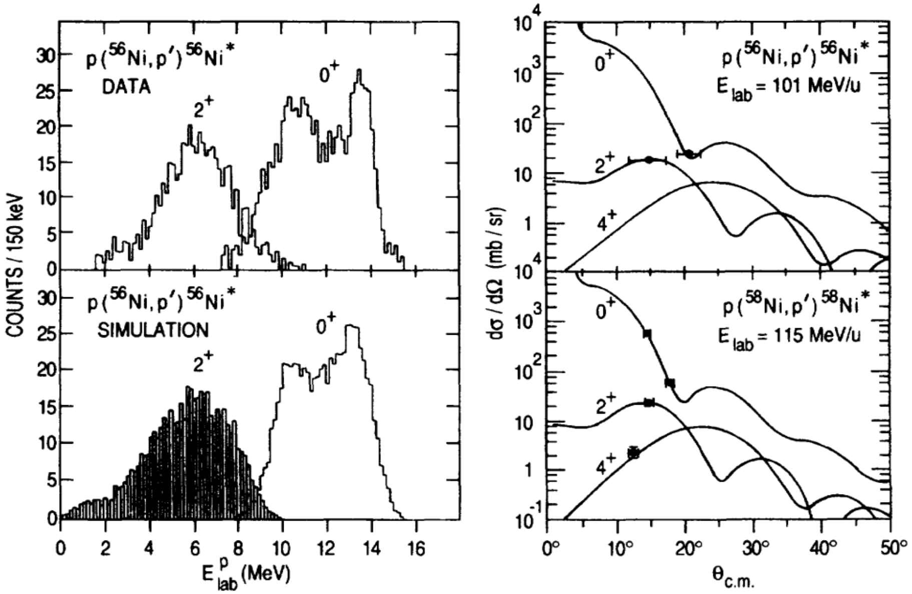

p(^{56}Ni,p') at GSI   energy resolution needed

G. Kraus et al., PRL ***73*** *(1994) 1773*

MUST Si-strip detector array at GANIL

Becheva et al., Phys. Rev. Lett. 96, 012501 (2006)

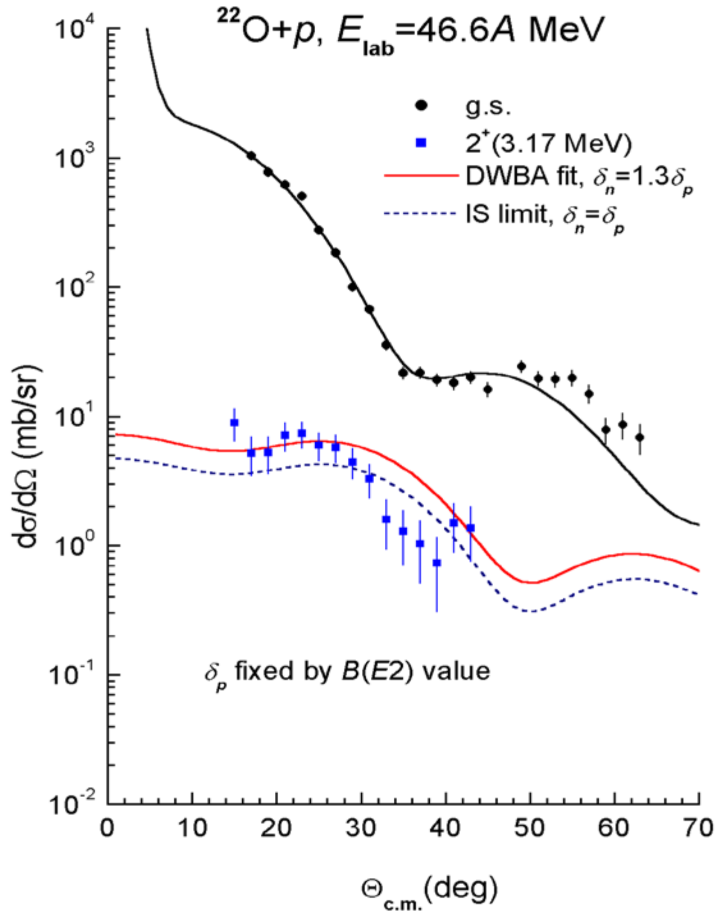

proton detection requires thin targets which limits ΔE to several hundred keV

low beam intensity is combined with thick target and γ-ray signal as tack for excited state & integrated cross section

Nucleon removal reactions

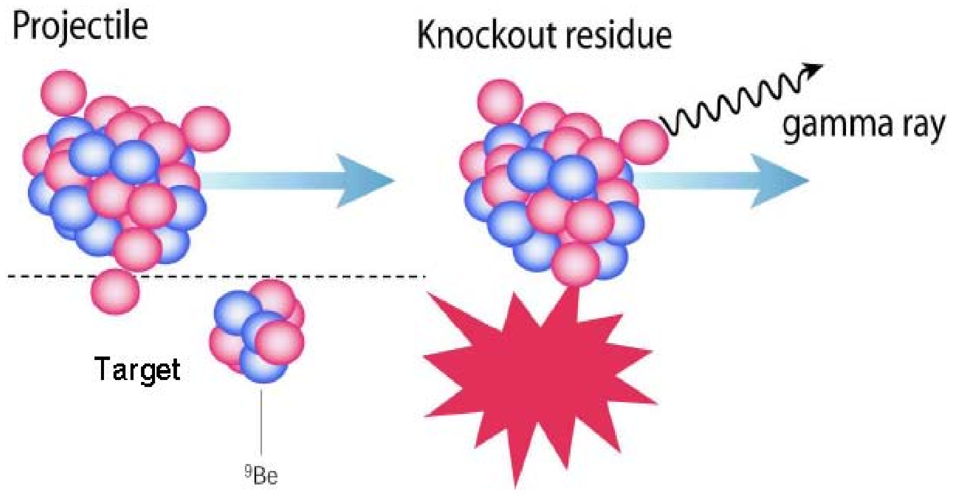

^{9}Be(^{11}Be, ^{10}Be + γ)X

Aumann, et al., Phys. Rev. Lett. 84, 35 (2000)

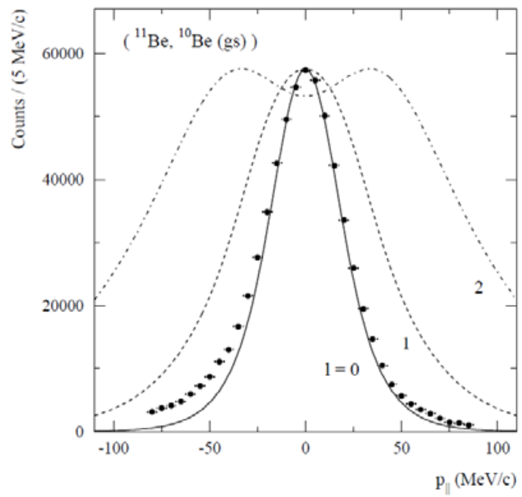

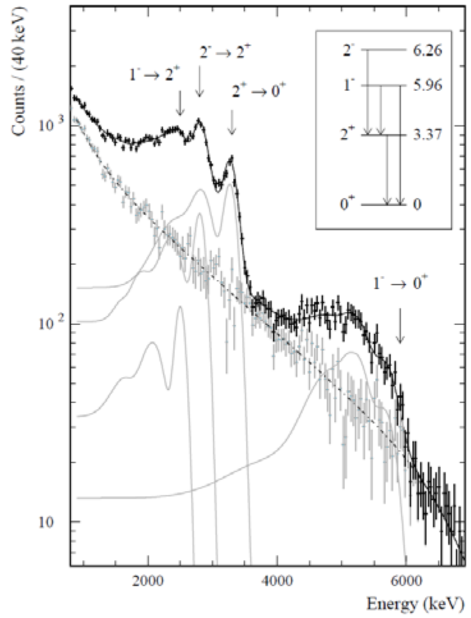

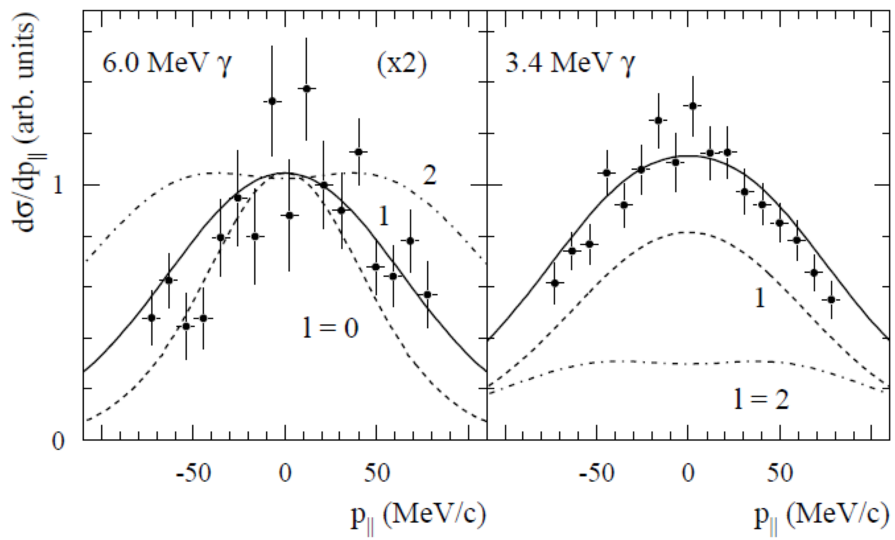

One-nucleon knockout schematics:
- neutron or proton is removed from projectile in single-step, direct reaction:
^{9}Be (^{A}Z, $^{A-1}$Z + γ)X or ^{9}Be (^{A}Z, $^{A-1}$Z-1 + γ)X.

- longitudinal momentum distribution of the heavy residue carries information on the orbital angular momentum (l-value) of the knocked-out nucleon
- analogy to angular distributions in low-energy transfer reactions.

–γ-ray spectroscopy in coincidence with projectile-like knockout residue for identification of final state.

- cross sections: 10 -140 mb

Direct two-nucleon knockout

New Direct Reaction: Two-Proton Knockout from Neutron-Rich Nuclei

D. Bazin et al, Phys. Rev. Lett. 91 (2003) 012501

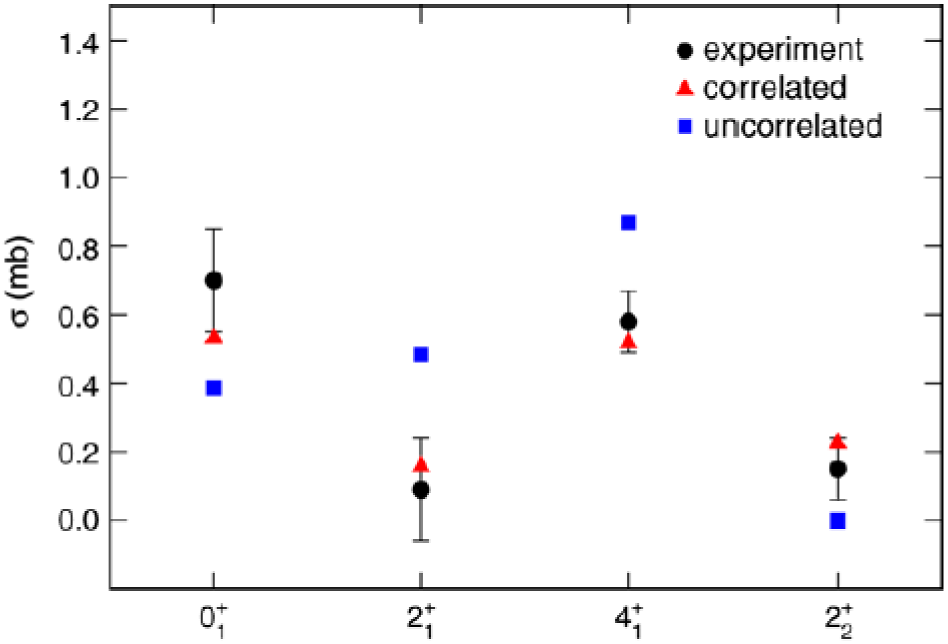

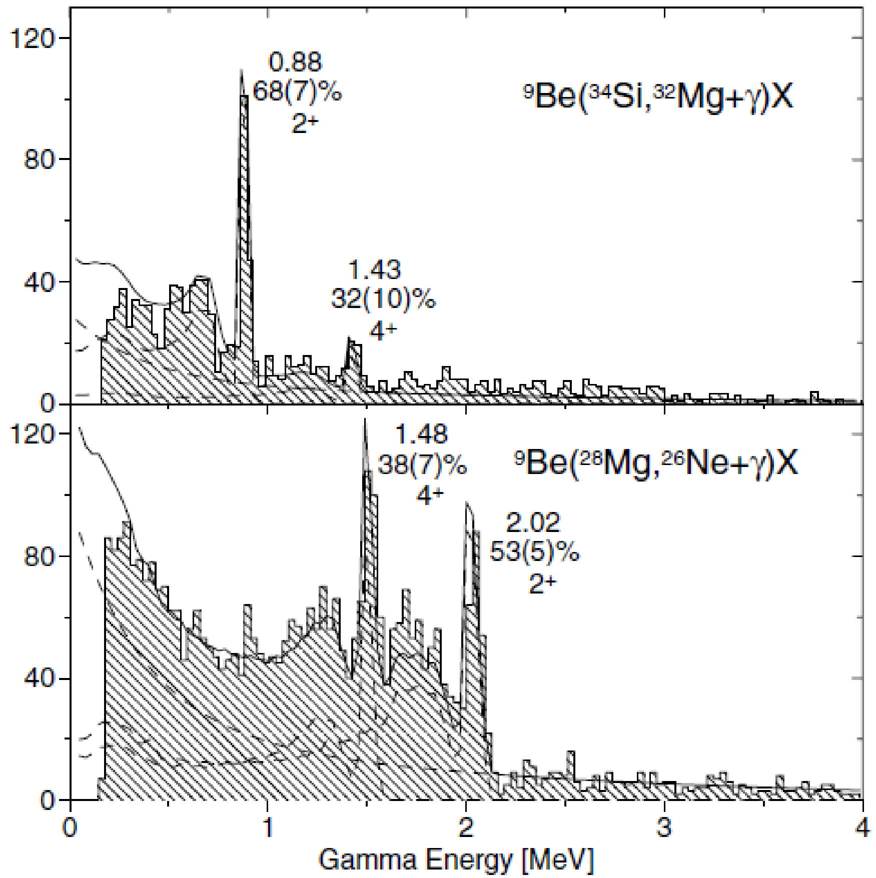

- partial cross sections for cross section to individual bound final states of residue provided by γ-ray spectroscopy
- many two-particle components contribute coherently for a given total angular momentum => associated interference effects
- strong interplay between nuclear structure and reaction dynamics
- ground state does not allow γ-ray identification, reconstructed by subtracting excited-state contributions.

Single-step and two-step fragmentation reactions

Two nucleon reactions

two-proton removal from neutron-rich nucleus → projectile-like residue even more neutron-rich

two-neutron removal from proton-rich nucleus → isotope even more neutron-deficient.

Secondary fragmentation

increased sensitivity in secondary fragmentation when neutron-rich or neutron-deficient projectiles induce fragmentation.

signal-to-noise ratio is enhanced in detection systems

weaker reaction channels leading to more exotic reaction products are accessible

Aim is first spectroscopy of most exotic nuclei

Example: secondary fragmentation of ^{36}Si at RIKEN

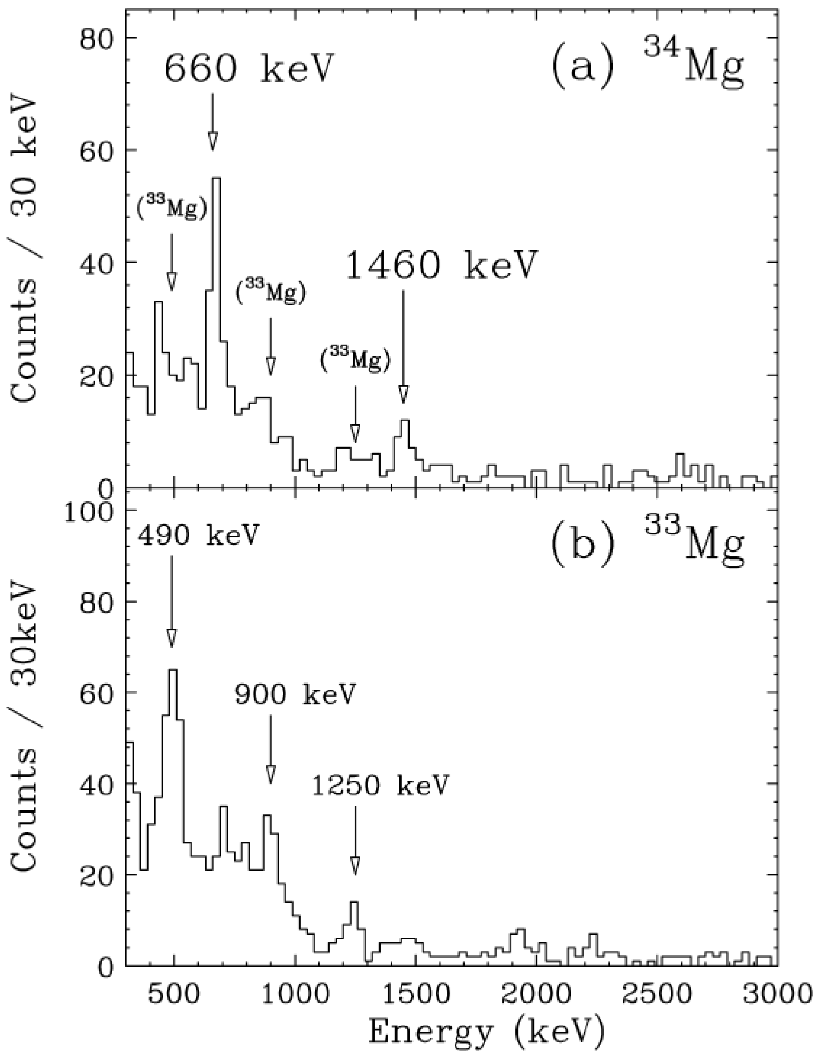

K. Yoneda et al. / Physics Letters B 499 (2001) 233–237

Intermediate-energy Coulomb excitation

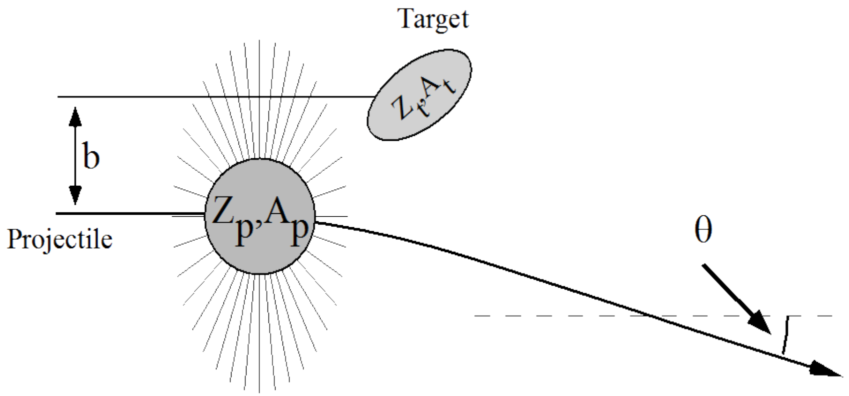

Excitation Cross Section

- projectile follows a Rutherford trajectory
- Coulomb excitation(CE) cross section is given by:

$$\left(\frac{d\sigma}{d\Omega}\right)_{\rm CE} = \left(\frac{d\sigma}{d\Omega}\right)_{\rm Ruth} P_{i\to f}\,,$$

probability of excitation from the initial state i to the final state f

electromagnetic interaction potential V(r(t)) treated as time-dependent perturbation:

$$P_{i\to f} = |a_{i\to f}|^2 \quad \text{with} \quad a_{i\to f} = \frac{1}{i\hbar}\int_{-\infty}^{\infty} e^{i\omega_{fi}t}\langle f|V(\boldsymbol{r}(t))|i\rangle\, dt\,.$$

The amplitudes $a_{i\text{-}f}$ can be expressed as a product of two factors

$$a_{i\to f} = i\sum_{\lambda}\chi^{(\lambda)}_{i\to f} f_\lambda(\xi)\,,$$

excitation strength χ is a measure of the strength of the interaction
f(ξ) measures the degree of adiabaticity -> ξ adiabaticity parameter

Intermediate-energy Coulomb excitation

Approximations:
Winther, Alder: static target & straight line trajectories

$$\gamma m_t v_t = \Delta p_\perp^{(t)} = \frac{2Z_t Z_p e^2}{b v_p} \qquad \theta_{\text{lab}} = \frac{2Z_t Z_p e^2}{\gamma m_p v_p^2} b^{-1}$$

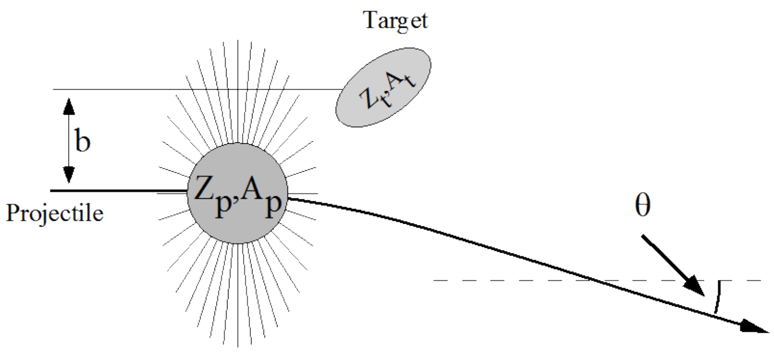

$Z_{p(t)}$ proton number of the projectile(target)
V_t incident projectile velocity
γ relativistic factor

b impact parameter
v_t target recoil velocity after collision.
m_t mass of the target nucleus

example:
$Z_t \sim 80$, $M_t \sim 200$ u $Z_p \sim 20$ heavy target, light exotic nucleus
Relativistic velocity: $v_p \sim 0{,}3$ c
Impact parameter: b = 15 fm
recoil velocities: $v_t < 0{,}2\%$ c

flight path of target nucleus: 0.1 fm compare to nuclear radius ~7 fm.

- target nucleus remains at rest during the collision process,
- coordinate system with target nucleus located (fixed) at the origin.
- detection angle of the projectile in the laboratory of a few degrees
- assumption of a straight-line trajectory justified

Intermediate-energy Coulomb excitation

Excitation Cross Section

Integration of excitation probability from a minimum impact parameter b_{min} (determined by experiment) to infinity. approx. result: use adiabatic cutoff and integration of absolute square of the excitation strength from b_{min} to b_{miax}

$$\sigma = 2\pi \int_{b_{\min}}^{\infty} P_{if}\, b db \approx 2\pi \int_{b_{\min}}^{b_{\max}} |\chi|^2\, b db$$

b_{max} can be estimated:

$$b_{\max} = \frac{\gamma v}{\omega_{fi}} = \frac{\gamma \hbar v}{\Delta E} \approx \frac{\gamma 197}{\Delta E} [MeV\ \ fm]$$

ΔE energy of the transition

Approximate expression for excitation cross section of parity π and multipolarity λ, assume bmax>>bmin

$$\sigma_{\pi\lambda} \approx \left(\frac{Z_t e^2}{\hbar c}\right)^2 \frac{\mathrm{B}(\pi\lambda, 0 \to \lambda)}{e^2} \pi b_{min}^{2(1-\lambda)} \cdot \begin{cases} (\lambda - 1)^{-1} & \text{for} \quad \lambda \geq 2 \\ 2\ln\left(\frac{b_{max}}{b_{min}}\right) & \text{for} \quad \lambda = 1\,, \end{cases}$$

$\mathrm{B}(\pi\lambda; 0 \to \lambda)$ is the reduced transition probability,

$$\begin{aligned} \mathrm{B}(\pi\lambda, I_i \to I_f) &= \sum_{\mu M_f} |\langle J_f M_f | \mathcal{M}(\pi\lambda\mu) | J_i M_i \rangle|^2 \\ &= \frac{1}{2J_i + 1} |\langle J_f \| \mathcal{M}(\pi\lambda) \| J_i \rangle|^2\,, \end{aligned}$$

$M(\pi\lambda\mu)$ multipole operator for electromagnetic transitions.

Intermediate-energy Coulomb excitation

• Excitation cross section is directly proportional to the reduced transition probability

$$\sigma_{i\to f} \propto B_t\left(\pi\lambda, I_i \to I_f\right)$$

B(πλ; 0 → λ) value can be extracted from cross section measurement

• Electric and magnetic fields of a moving charge related through:

$$\left|\vec{B}\right| = \frac{v}{c}\left|\vec{E}\right|$$

for high-energy relativistic Coulomb excitation, of interest here, (v/c >0.3) magnetic excitations are possible and must be considered

• Exact expression for the excitation cross section, summed over parities and multipolarities:

$$\sigma_{i\to f} = \left(\frac{Z_p e^2}{\hbar c}\right)^2 \sum_{\pi\lambda\mu} k^{2(\lambda-1)} \frac{B_t\left(\pi\lambda, I_i \to I_f\right)}{e^2} \left|G_{\pi\lambda\mu}\left(\frac{c}{v}\right)\right|^2 g_\mu\left(\xi\left(b_{\min}\right)\right)$$

Intermediate-energy Coulomb excitation

Three Basic Parameters

Impact Parameter and Distance of Closest Approach

$$\theta_{\text{lab}} = \frac{2Z_t Z_p e^2}{\gamma m_p v_p^2} b^{-1}$$

- relates impact parameter b and detection angle in the laboratory
- straight-line trajectories are a good approximation
- distance of closest approach is nearly equal to the impact parameter
- has to be larger than the sum of two nuclear radii to ensure dominance of Coulomb excitation:

Minimum distance is ensured experimentally by limiting the scattering angle of the projectile below a certain maximum scattering angle

$$\theta \leq \theta_{\max} \Rightarrow b \geq b_{\min}\left(\theta_{\max}\right)$$

Intermediate-energy Coulomb excitation

Basic Parameters

Sommerfeld Parameter

$$\eta = \frac{b}{\lambda\!\!\!^{-}} = \frac{b\gamma m_p v_p}{\hbar} \qquad \text{with} \quad \gamma = \frac{1}{\sqrt{1-\beta^2}} \quad \text{and} \quad \beta = \frac{v_p}{c}$$

compares the physical dimensions of the classical orbit the impact parameter b,
with the de Broglie wavelength of the relative motion of the two particles

typical values are ~1000, implying that a wave packet containing several waves is still small compared to the dimensions of the trajectory.

wave packet will move along the classical trajectory, justifying the use of the semi-classical approach in the calculation of the Coulomb excitation cross section.

Intermediate-energy Coulomb excitation

Basic Parameters

Adiabaticity Parameter

If the time-dependent perturbation potential changes slowly the nucleus follows the perturbation adiabatically and no excitation is possible
→ adiabatic cutoff

$$\xi = \frac{\tau_{coll}}{\tau_{nucl}}$$

a) collision time is short enough for adiabaticity parameter to be small and excitations are possible
Classical picture: force vectors acting on the deformed cause a torque and generate excitations

b) nucleus follows motion of the projectile, no torque is generated and no excitations occur,

the field strengths are similar in both cases.

ξ is large then no excitation is possible
- projectile velocity is low
- impact parameter is large.

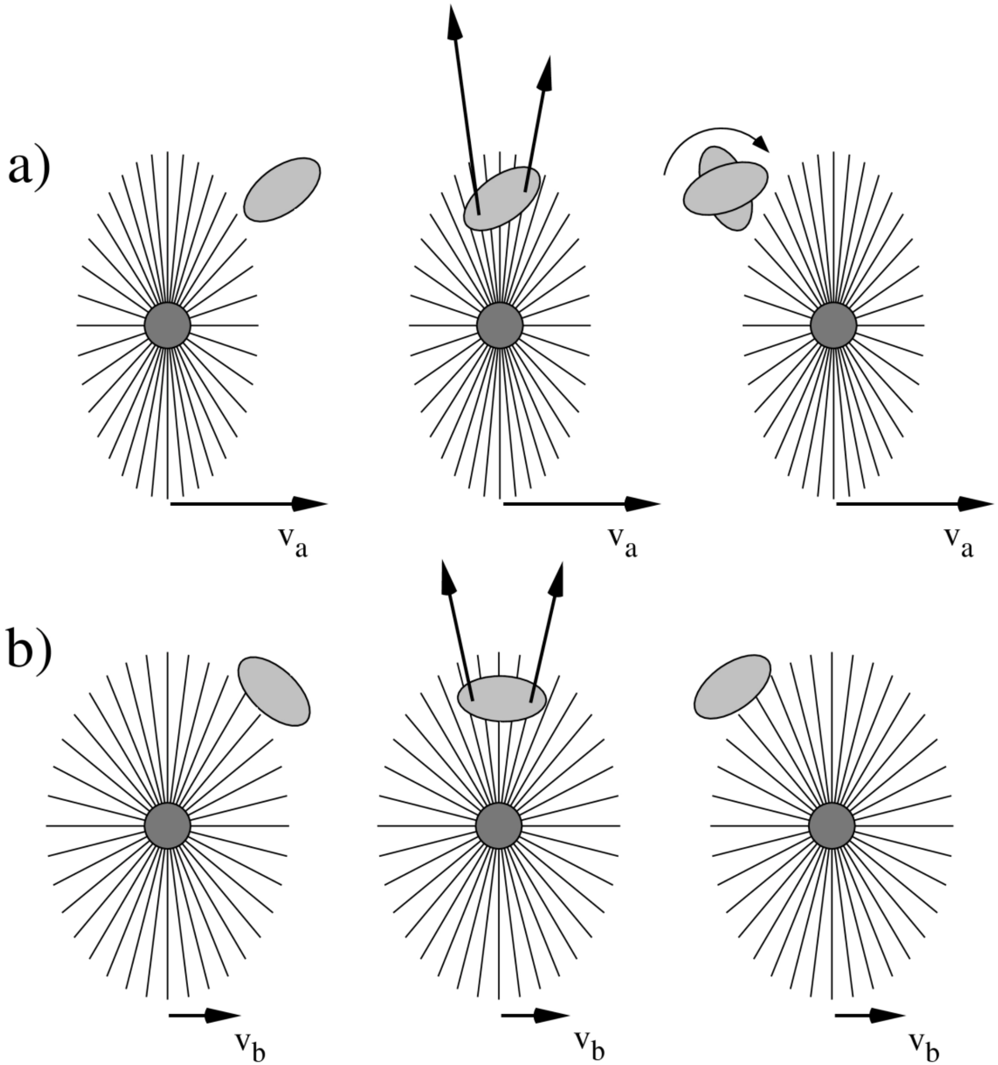

Intermediate-energy Coulomb excitation

Adiabaticity Parameter

electric field component in the x-direction E_x (perpendicular to the direction of motion) produced by the projectile at the target position:

$$E_x = \frac{\gamma E_0}{\left(1+\left(t^2/\tau^2\right)\right)^{3/2}} \quad \text{with} \quad \tau = \frac{b}{\gamma v_p} \quad \text{and} \quad E_0 = \frac{eZ_p}{b^2}$$

collision time is given by τ

time scale for the nuclear motion is given by ωif=ħ/ΔE

$$\xi = \omega_{fi}\frac{b}{\gamma v_p} = \frac{\Delta E b}{\hbar \gamma v_p}$$

e.g. with β~0.3 and b=15 fm ξ~ ΔE/5MeV

for higher β values higher excitation energies

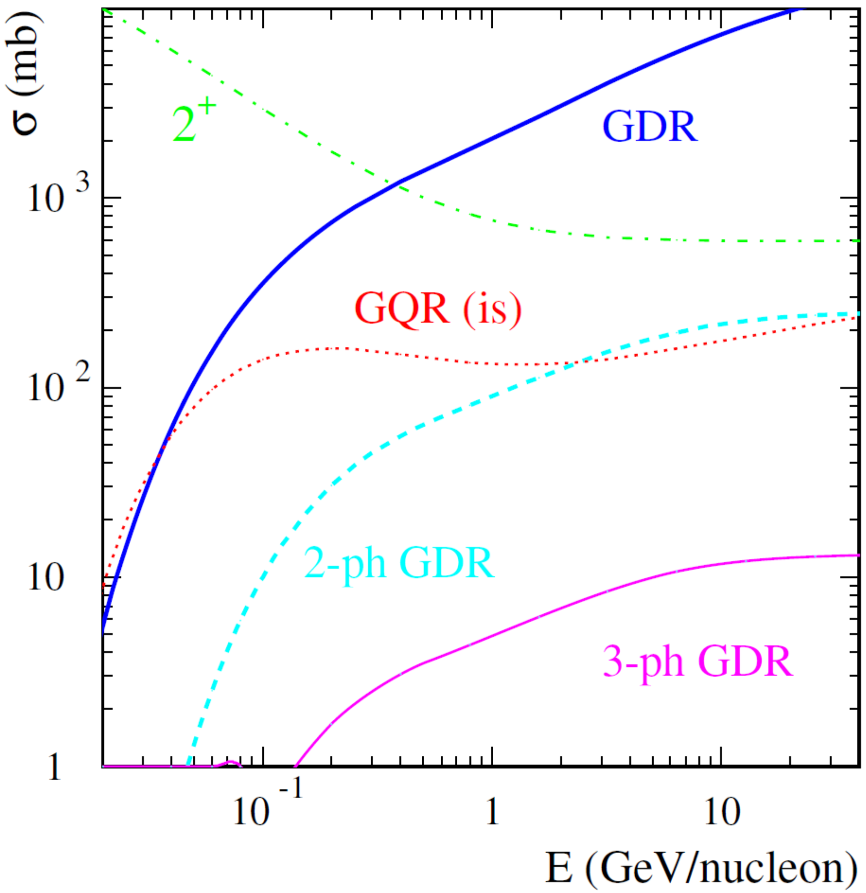

Intermediate-energy Coulomb excitation

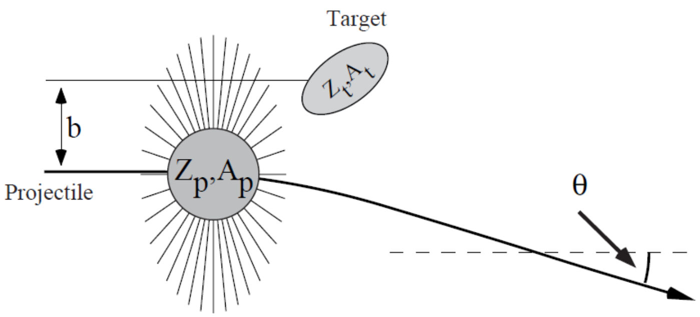

Equivalent Photon Method

Coulomb excitation can be viewed as absorption of virtual photons by the target nucleus.
Virtual photons are produced by the moving projectile.
Equivalent photon number (the number of real photons that would have an equivalent net effect for one particular transition) is related to the *Fourier transform of the time-dependent electromagnetic field produced by the projectile.*

Coulomb excitation cross section

$$\sigma_{i\to f} = \sum_{\pi\lambda} \int N_{\pi\lambda}(\omega)\sigma_\gamma^{(\pi\lambda)}(\omega)\frac{d\omega}{\omega},$$

spectrum of photons of multipolarity π,λ determined by photoabsorption cross section σ

$$\sigma_\gamma^{(\pi\lambda)}(\omega) = \frac{(2\pi)^3(\lambda+1)}{\lambda((2\lambda-1)!!)^2}\,\rho(\epsilon)k^{2\lambda+1}B(\pi\lambda),$$

$\rho(\varepsilon)$ is the density of final states is δ-function for discrete nuclear states

number of equivalent photons $N_{\pi,\lambda}(\omega)$ of multipolarity π,λ

$$N_{\pi\lambda}(\omega) = Z_p^2\frac{e^2}{\hbar c}\frac{l((2l+1)!!)^2}{(2\pi)^3(\lambda+1)}\sum_\mu \left|G_{\pi\lambda\mu}\left(\frac{c}{v}\right)\right|^2 g_\mu(\xi).$$

Intermediate-energy Coulomb excitation

- active programs at GANIL, GSI, MSU and RIKEN
- one-step process
- sensitive to *E*1, *E*2, *E*3 excitations
- accurate technique that allows for absolute B(E2) measurements

Comparison with different methods, comparison for different nuclei

Adopted and measured
B(E2) values for stable nuclei

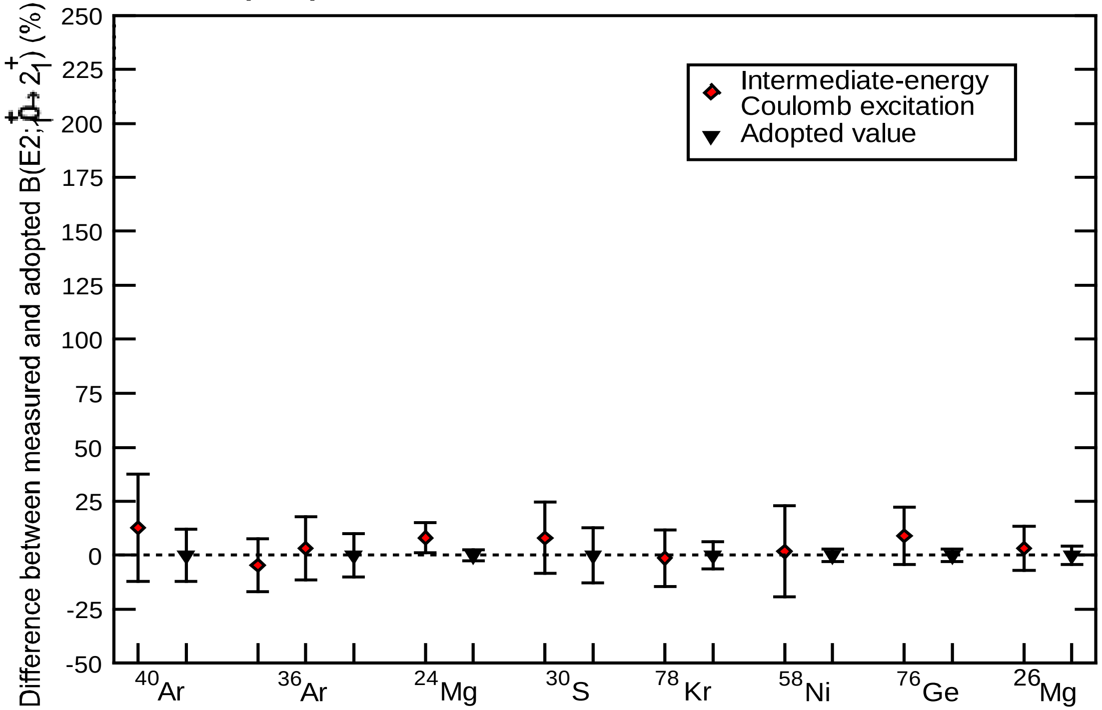

B(E2) values from
different methods for ^{26}Mg

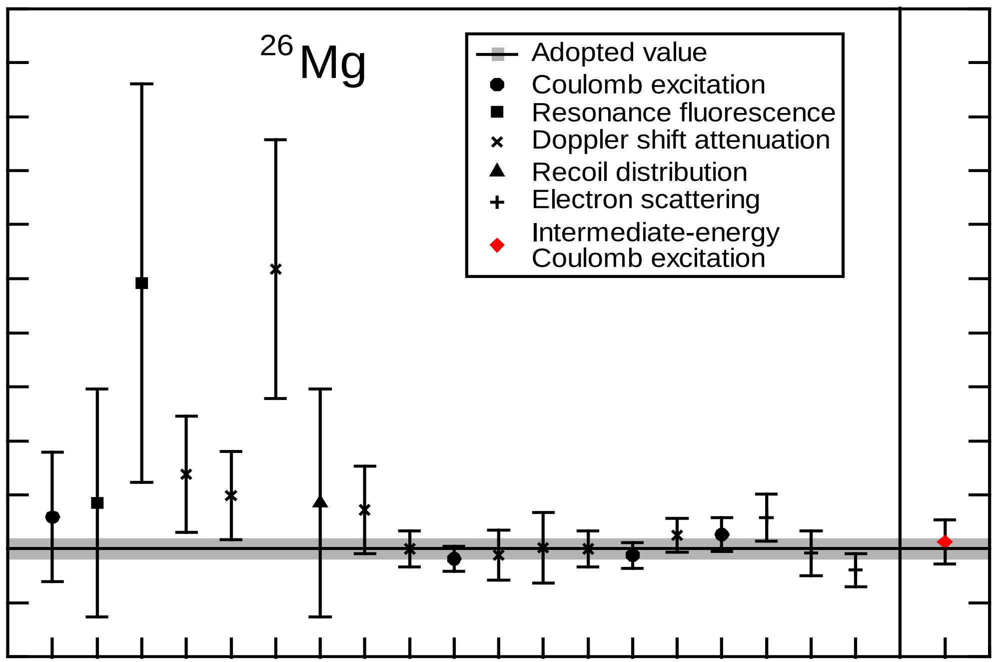

J. Cook et al., Phys. Rev. ***C 73*** *(2006) 024315*

Shell structure in exotic sd-shell nuclei

Deviations from classical shell model

Frontiers and challenges of nuclear shell model

T. Otsuka *et al.*, Euro. Phys. Journal A **15**, 151 (2002)

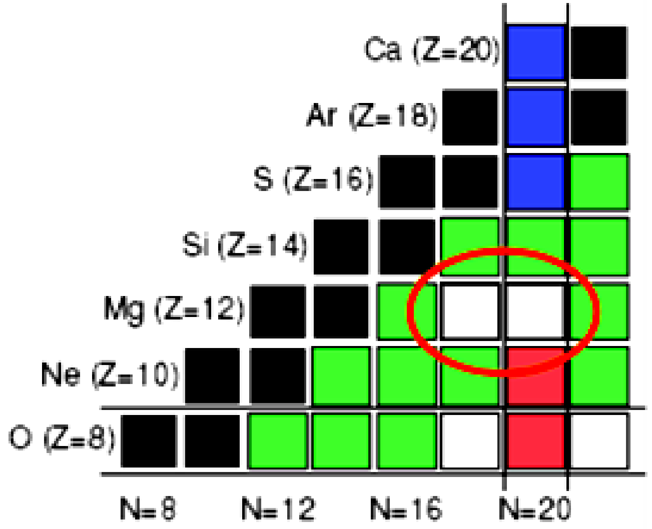

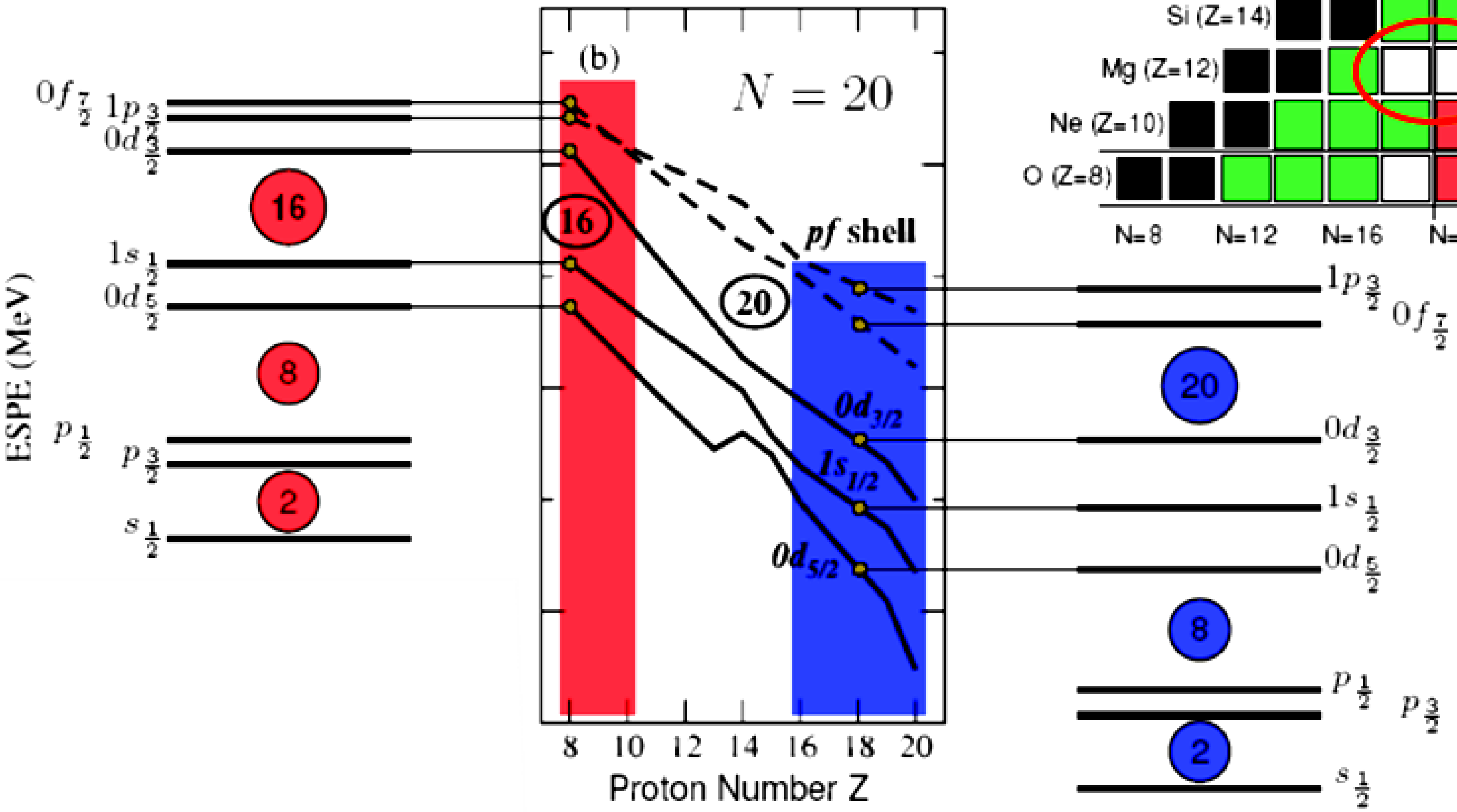

Island of inversion

1975, ISOLDE: C. Thibault *et al.*:
Masses show considerable deviations for nuclei around Z=11, N=20.
⇒ additional binding energy

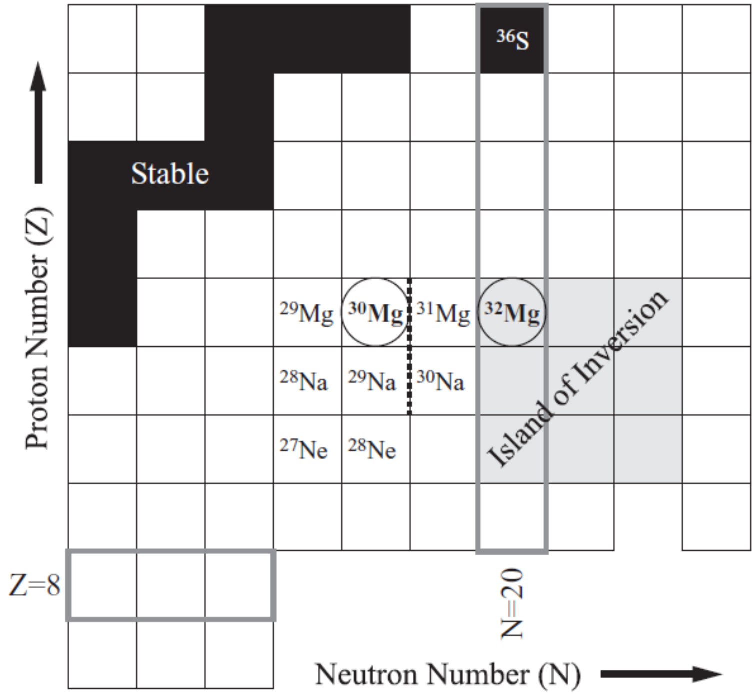

Normal *sd*-shell configuration

0p0h, spherical

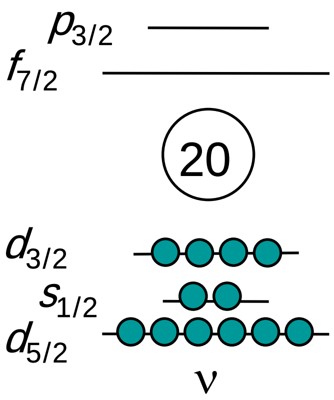

2p2h (intruder), deformed

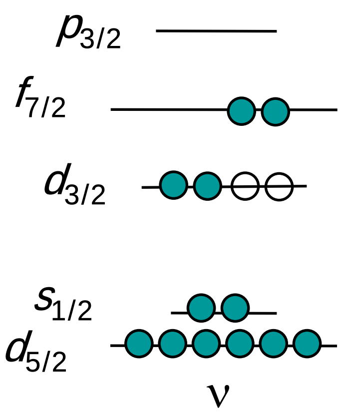

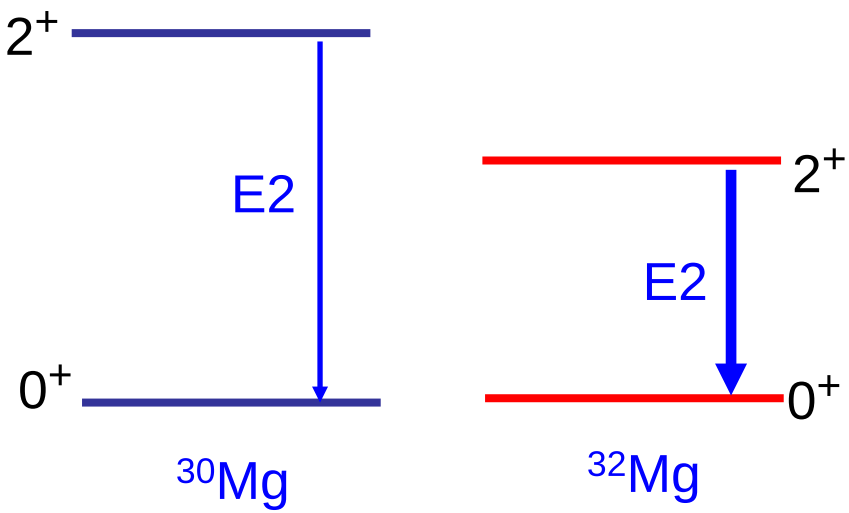

E.K. Warburton, J. A. Becker and B. A. Brown, PRC **41** (1990) 1147.

T. Motobayashi, et al.; PLB **346** (1995) 9

Island of Inversion: At the border and beyond

P. Doornenbal, et al; PRL 103, 032501 (2009)

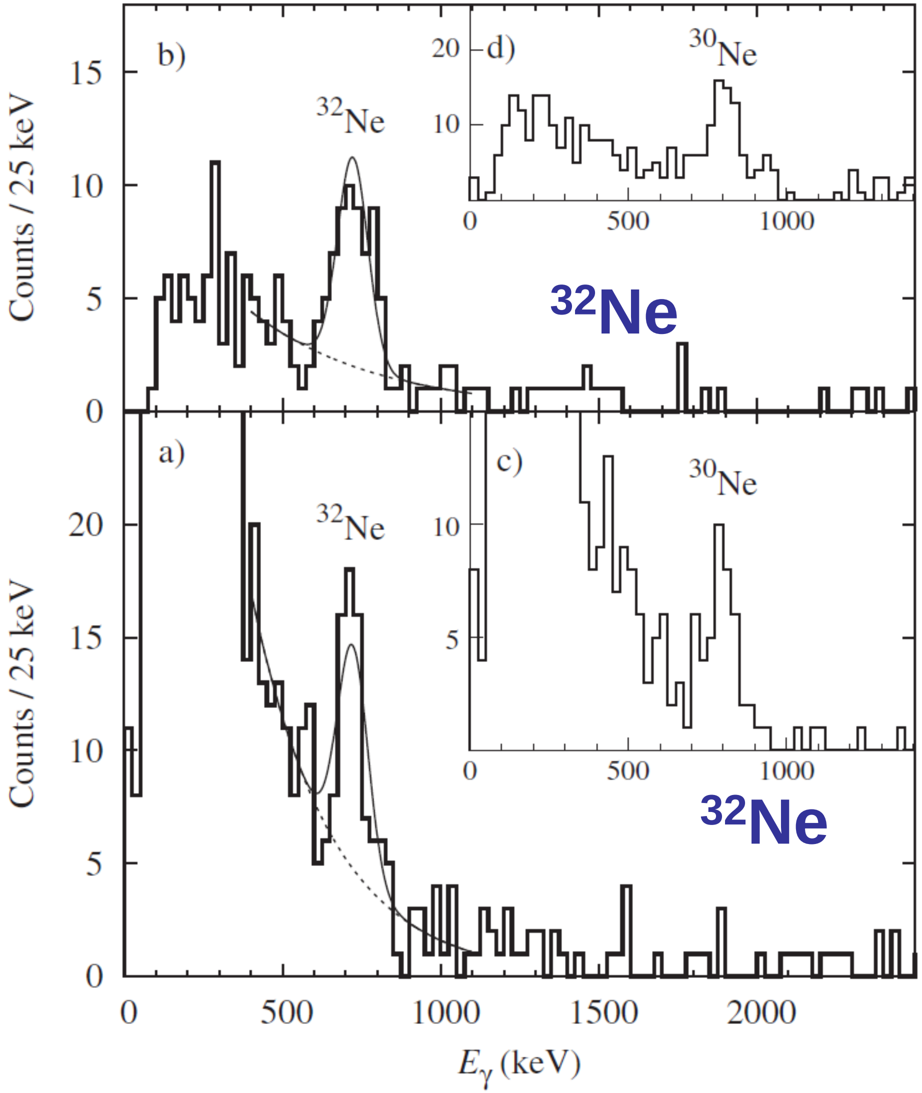

A. Gade, et al; PRL 99, 072502 (2007)

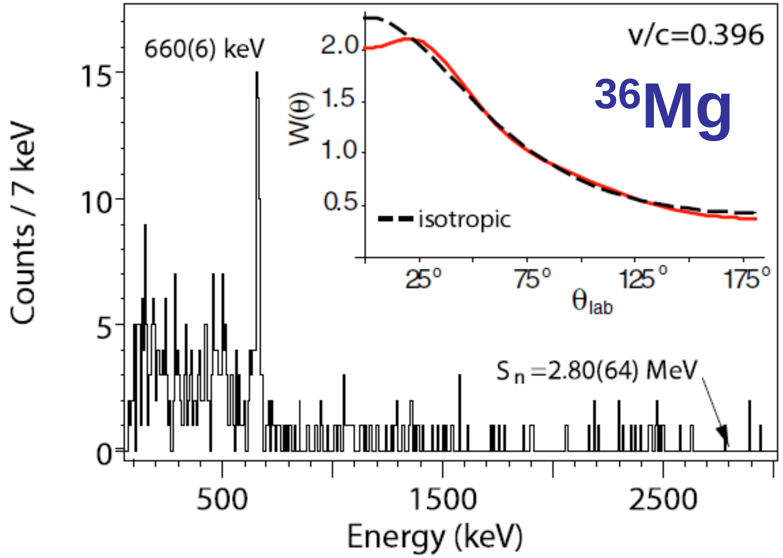

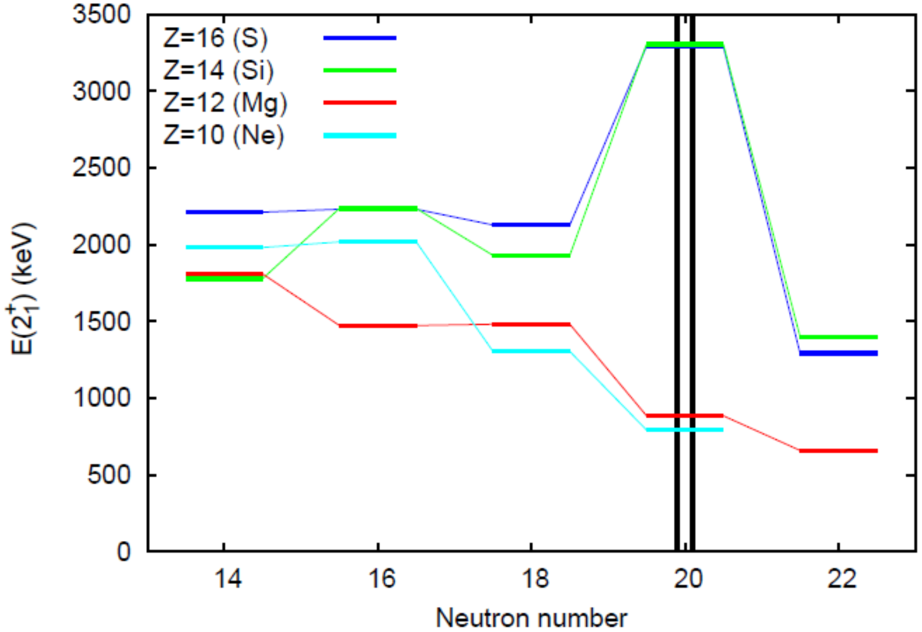

Island of Inversion

Results of intermediate Coulomb excitation experiments
Status 2004

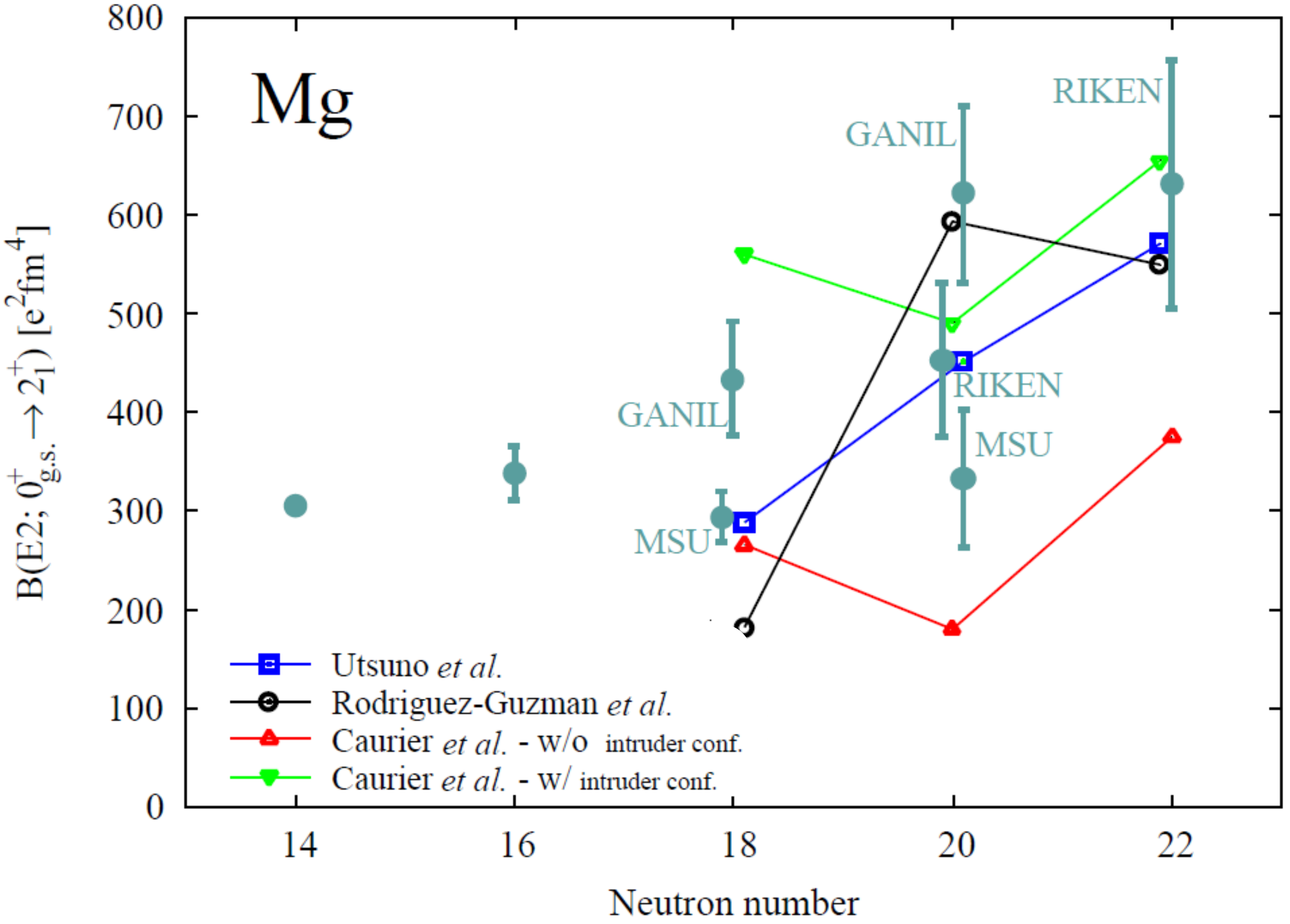

A different approach: Safe Coulomb excitation

but instable radioactive ion beams

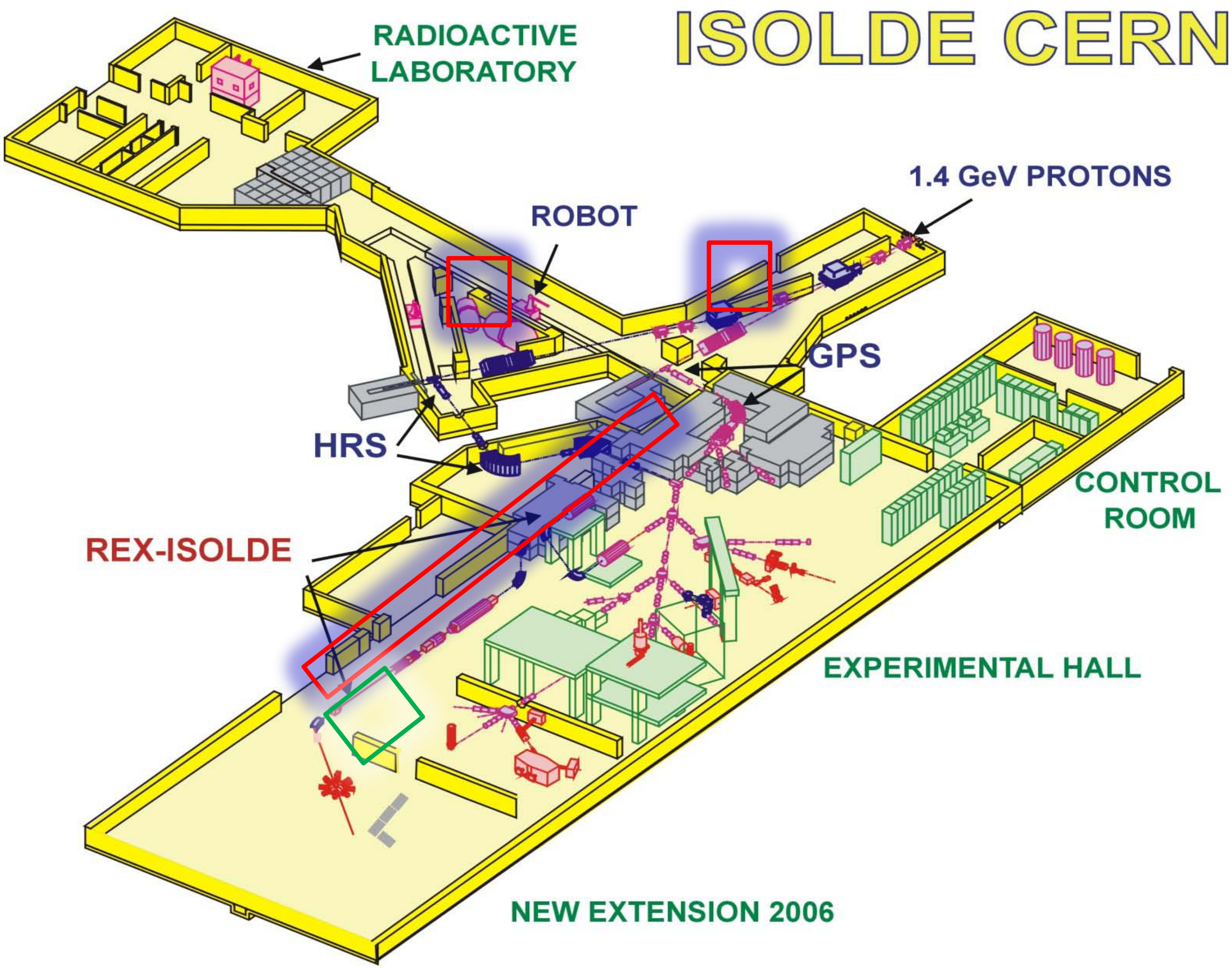

- Energy of the nuclear levels
- Probability of the transition (BE2)
- Multipolarity of the transition (E2, M1)

$$\left(\frac{d\sigma_{CE}}{d\Omega}\right)_n = \left(\frac{d\sigma_{Ruth}}{d\Omega}\right) \cdot P_n$$

where $P_n = \left|a_n\right|^2$

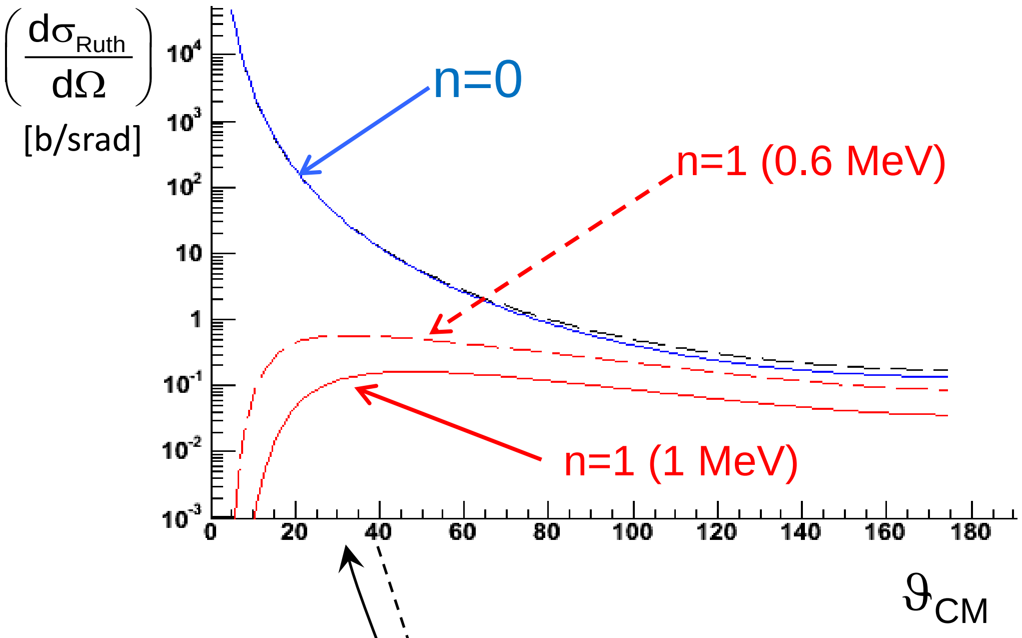

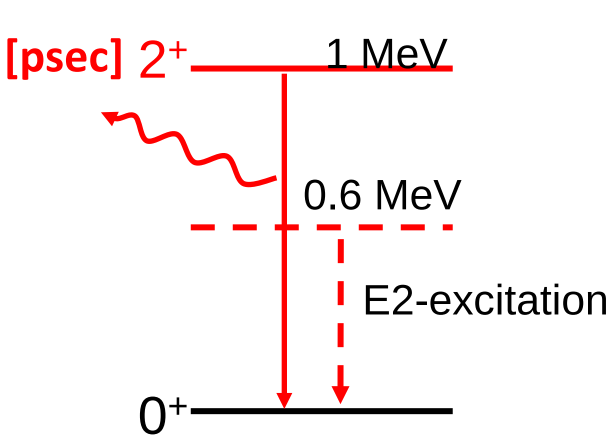

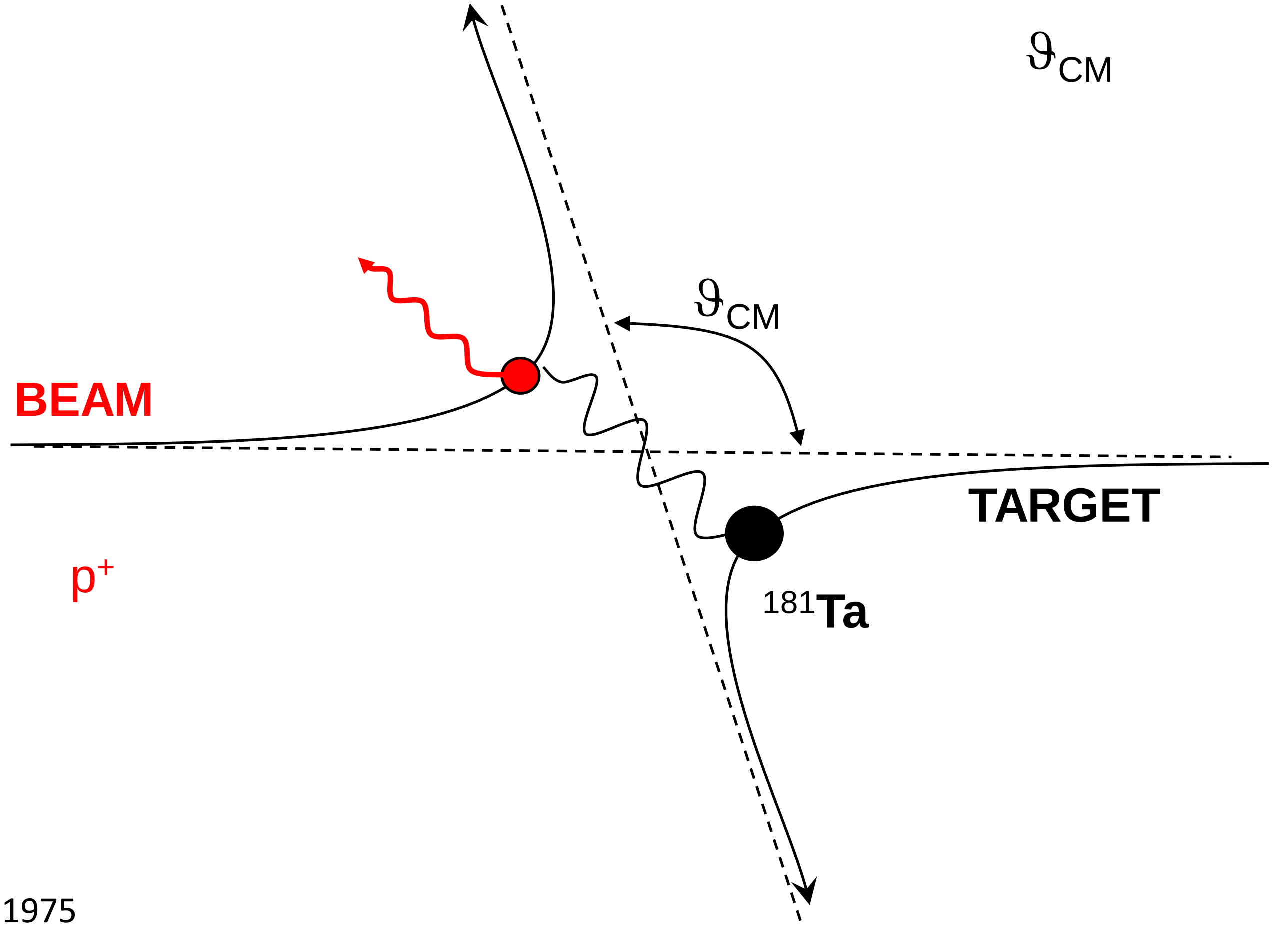

Alder-Winter, Theory of Coulomb excitation with heavy ions, 1975

Energy of the nuclear levels ;
Probability of the transition (BE2) ;
Multipolarity of the transition (E2, M1) ;

$$\left(\frac{d\sigma_{CE}}{d\Omega}\right)_n = \left(\frac{d\sigma_{Ruth}}{d\Omega}\right) \cdot P_n$$

where $P_n = |a_n|^2$

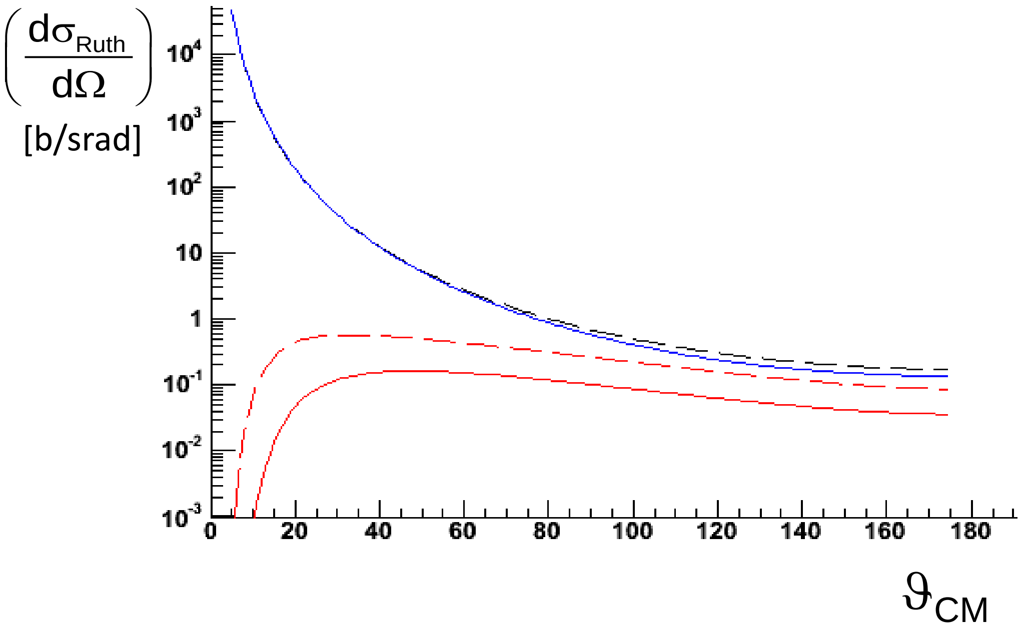

$\sigma_{CE} \sim B(E2)$

with $B(E2, J_i \rightarrow J_f) = (2Ji+1)^{-1} . |\langle J_i || E2 || J_f \rangle|^2$

Alder-Winter, Theory of Coulomb excitation with heavy ions, 1975

Energy of the nuclear levels ;
Probability of the transition (BE2) ;
Multipolarity of the transition (E2, M1) ;

$\sigma_{CE} \sim B(E2)$

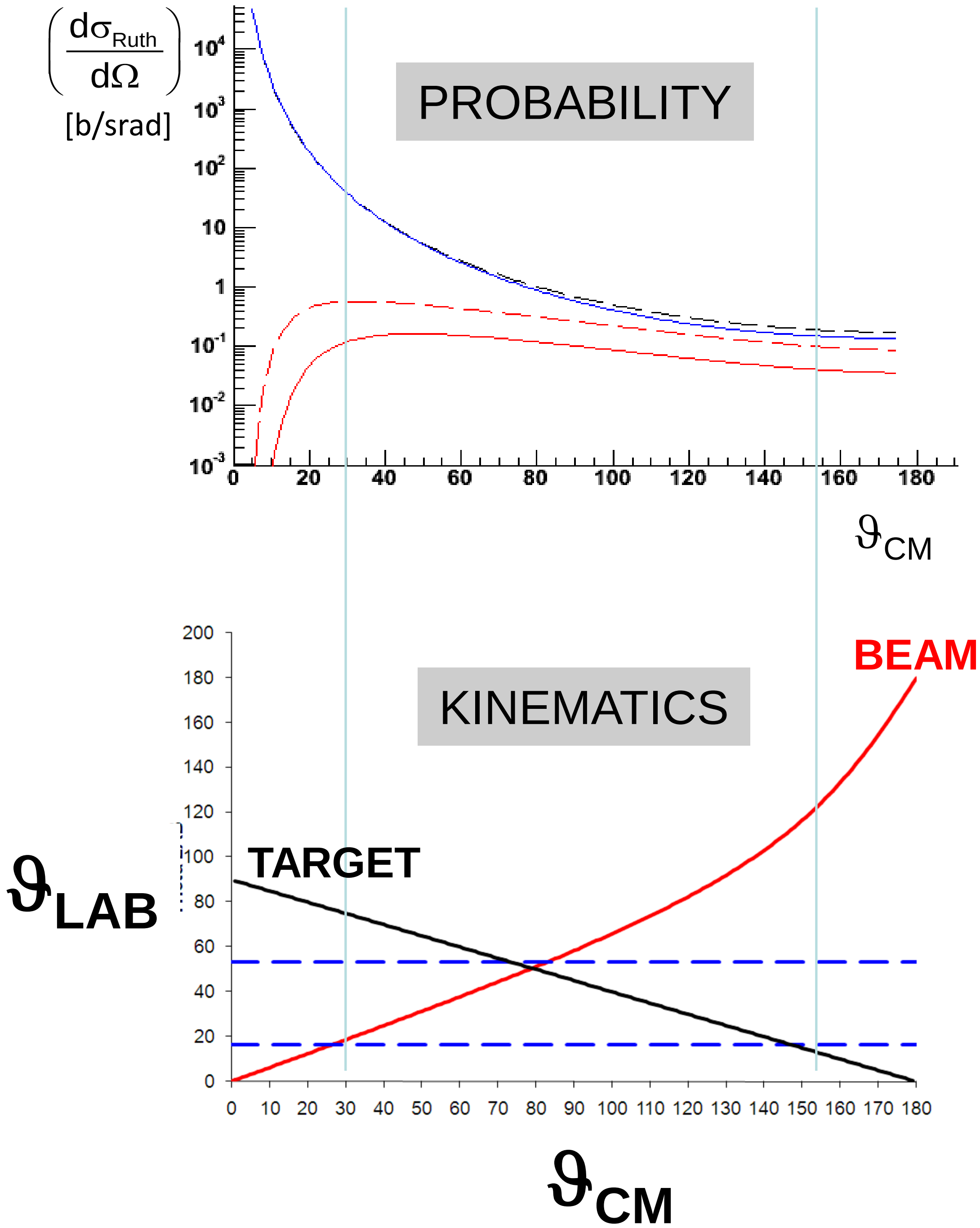

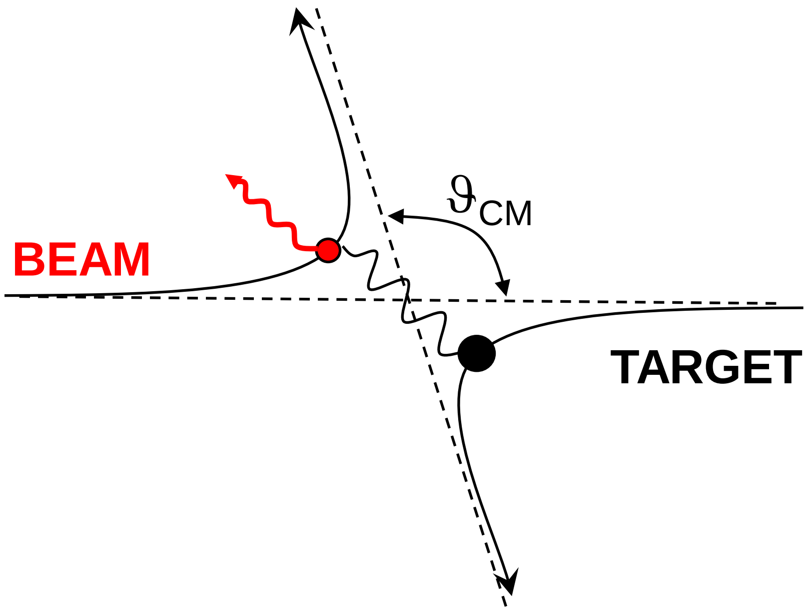

Mass beam < Mass Target

Alder-Winter, Theory of Coulomb excitation with heavy ions, 1975

Energy of the nuclear levels ;
Probability of the transition (BE2) ;
Multipolarity of the transition (E2, M1) ;

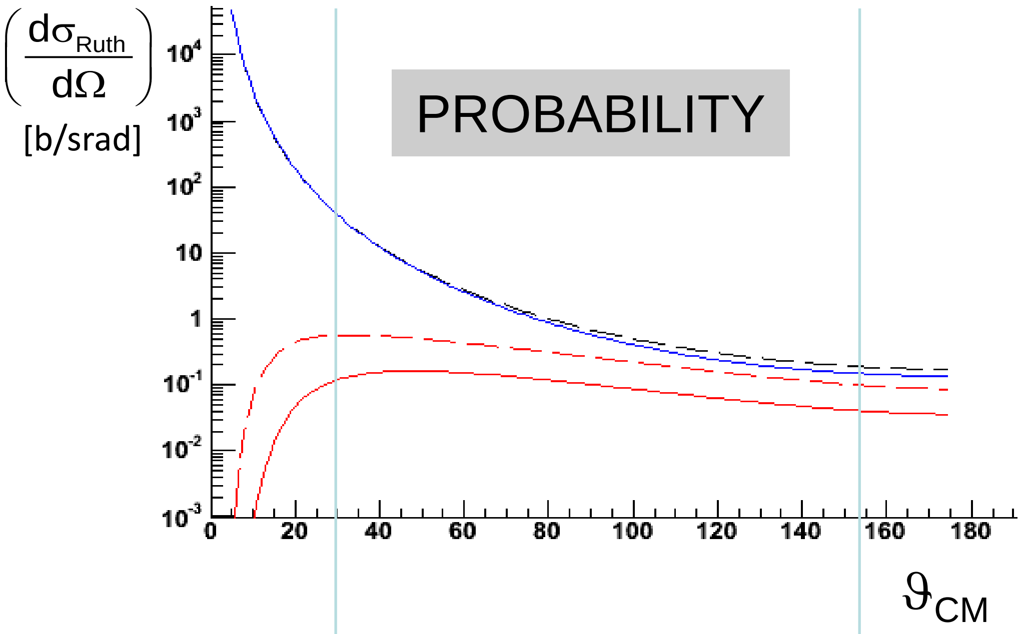

$\sigma_{CE} \sim B(E2)$

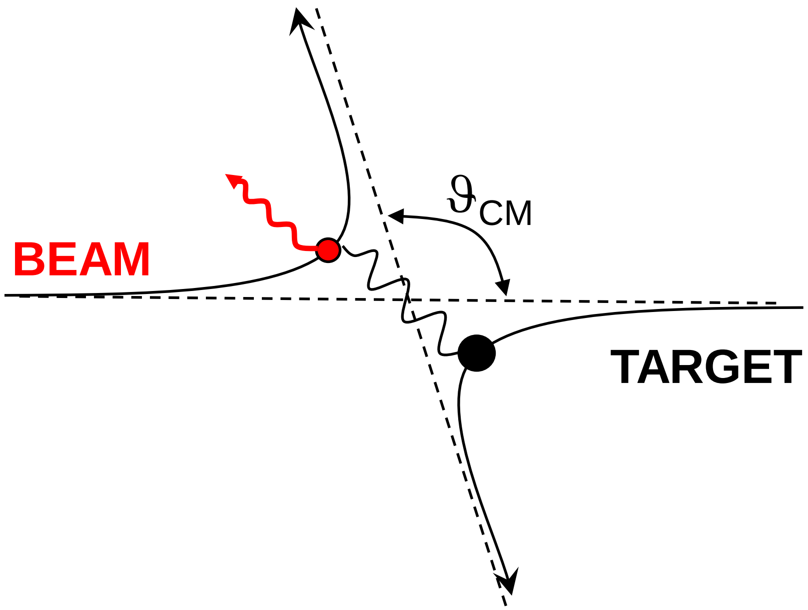

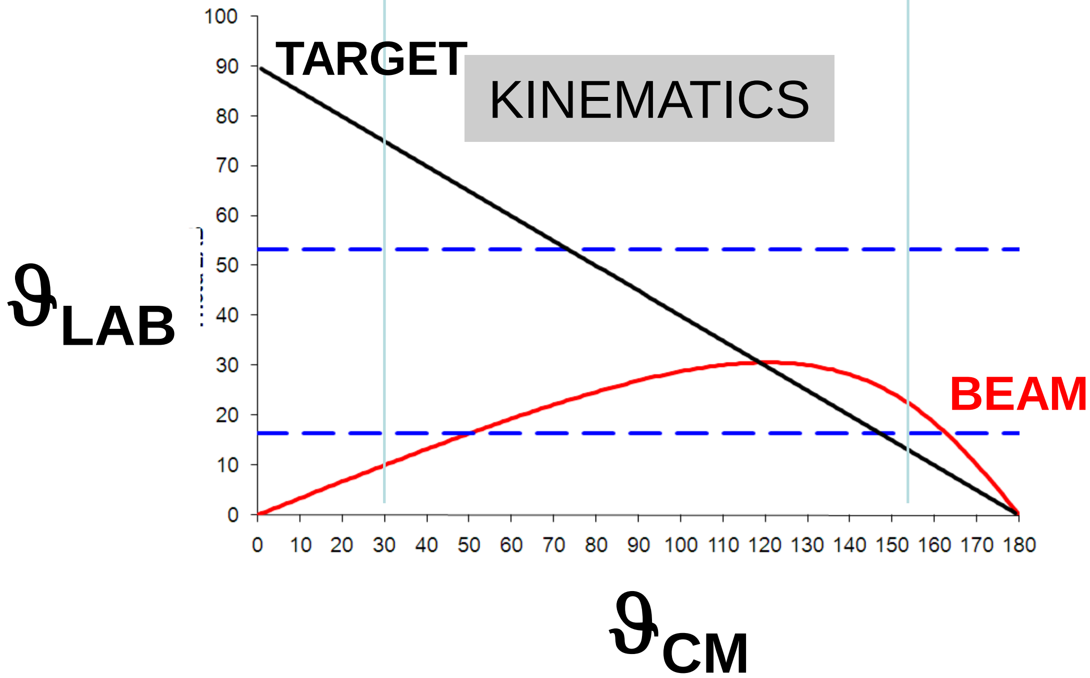

Mass beam > Mass Target

Alder-Winter, Theory of Coulomb excitation with heavy ions, 1975

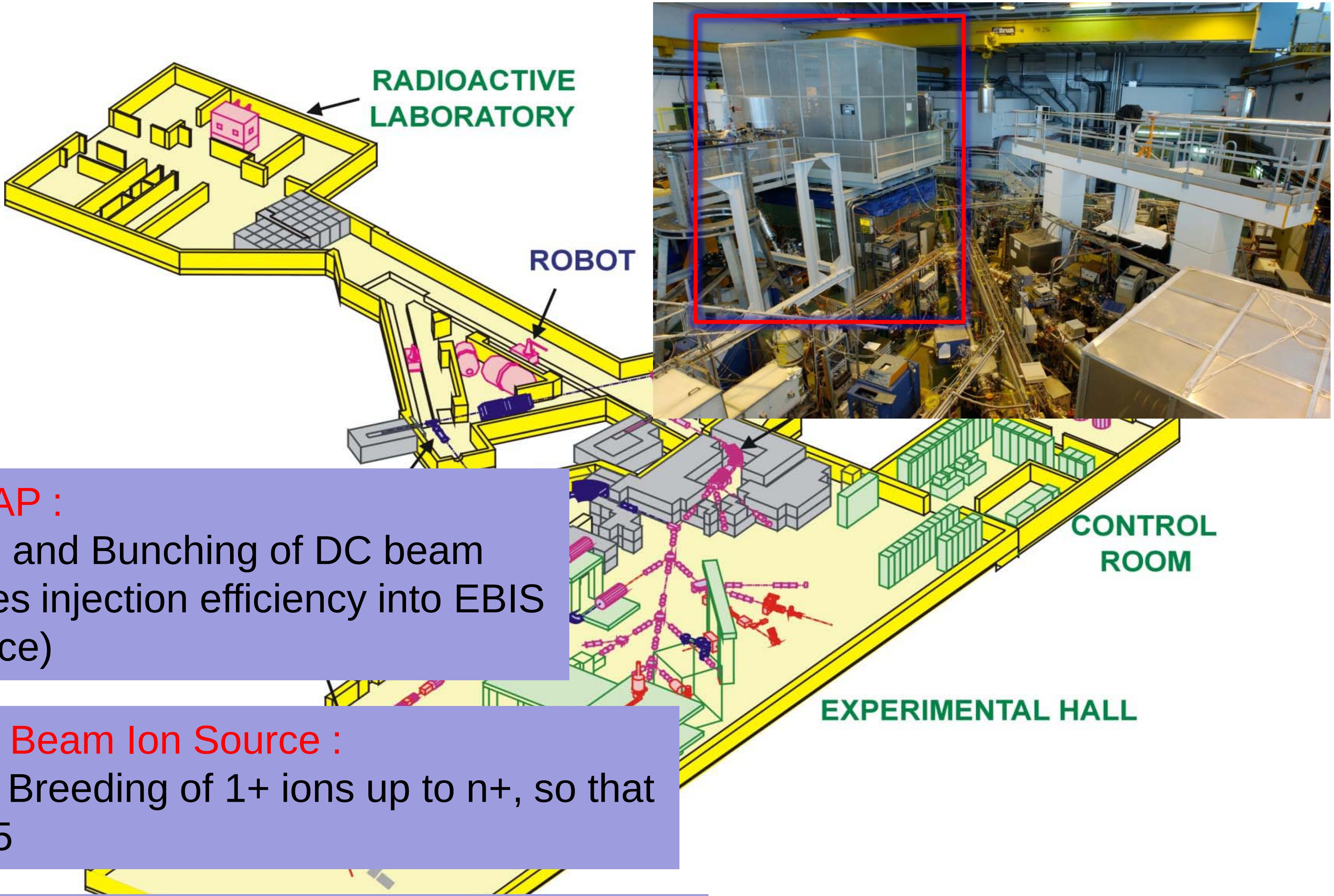

REXTRAP :

-Cooling and Bunching of DC beam

-Improves injection efficiency into EBIS (emittance)

Electron Beam Ion Source :

-Charge Breeding of 1+ ions up to n+, so that A/q < 4.5

POST ACCELERATION :

-limited in length -> high charge state needed !

-NOT continuously on -> bunched beam !

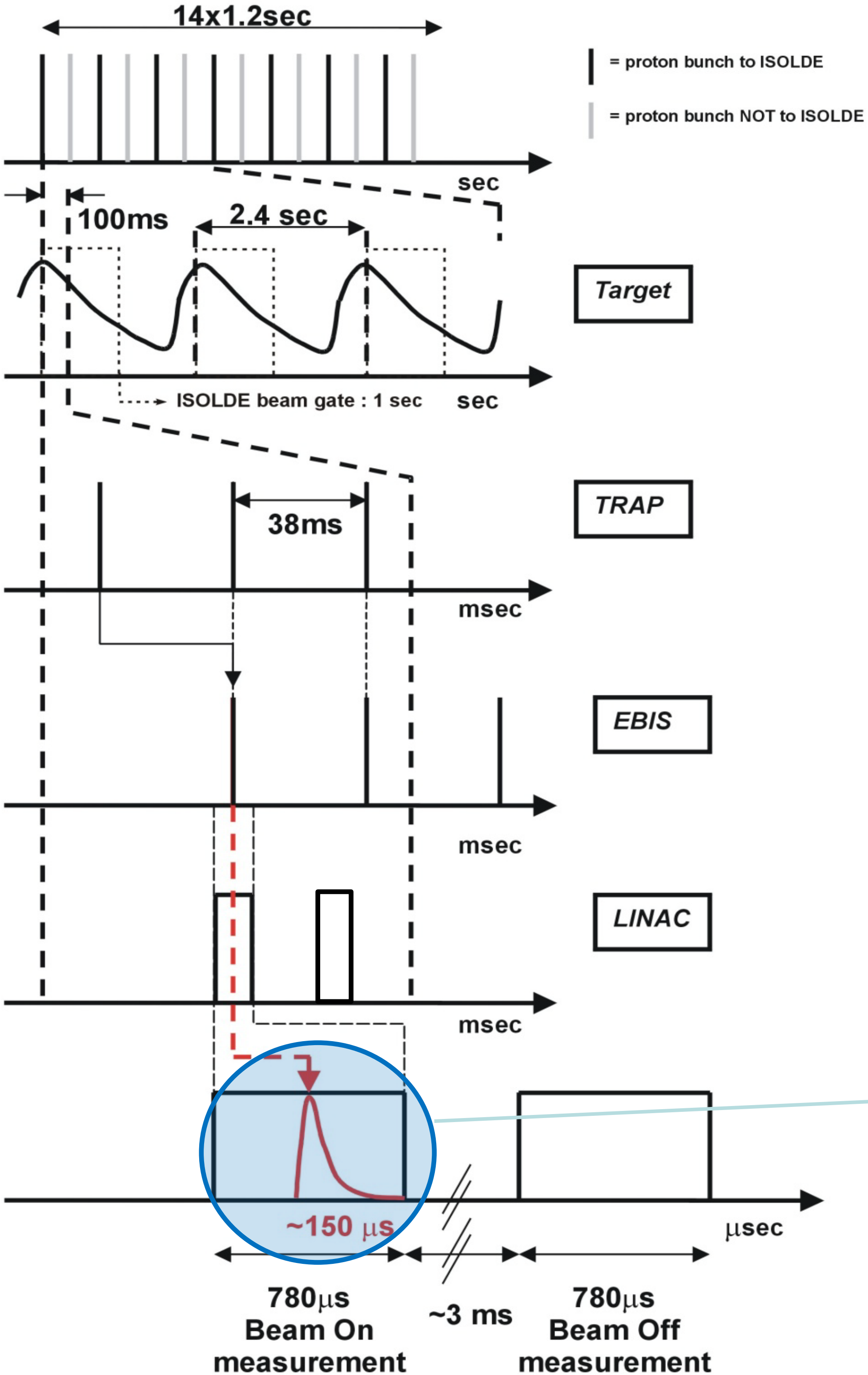

14x1.2sec
= proton bunch to ISOLDE
= proton bunch NOT to ISOLDE
sec
100ms
2.4 sec
Target
ISOLDE beam gate : 1 sec
sec
TRAP
38ms
msec
EBIS
msec
LINAC
msec
~150 µs
µsec
780µs
Beam On
measurement
~3 ms
780µs
Beam Off
measurement

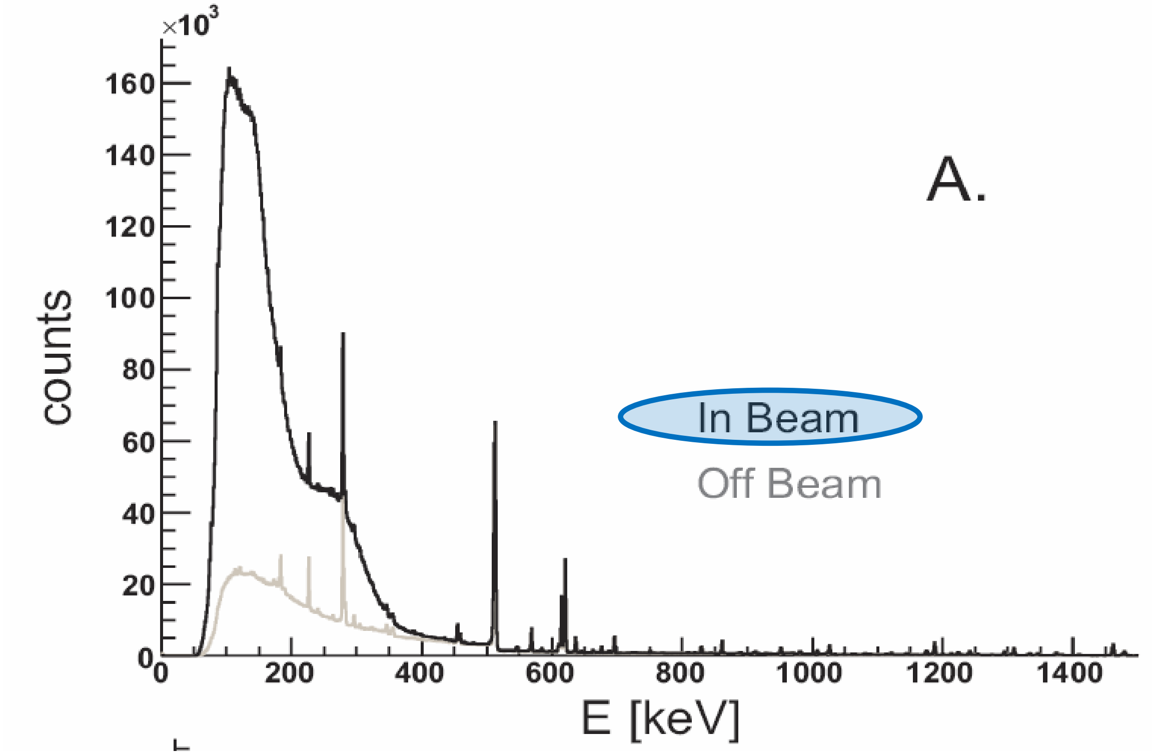

×10³
160
140
120
100
80
60
40
20
0
counts
0
200
400
600
800
1000
1200
1400
E [keV]
A.
In Beam
Off Beam

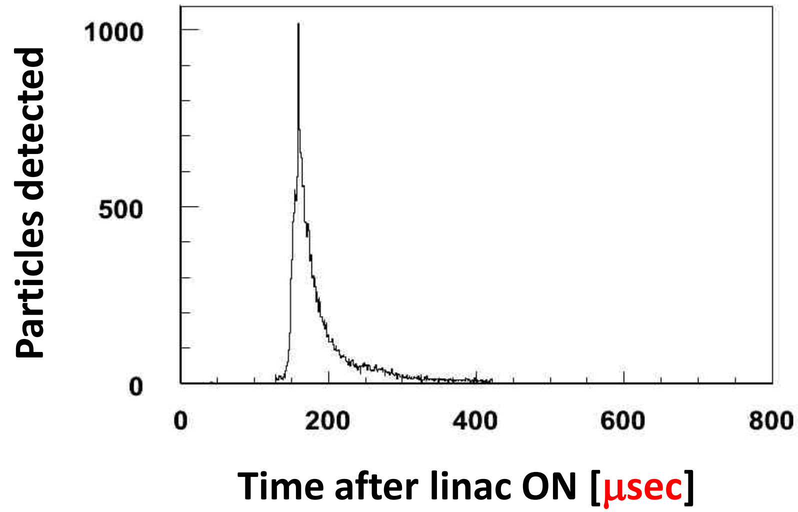

1000
500
0
Particles detected
0
200
400
600
800
Time after linac ON [µsec]

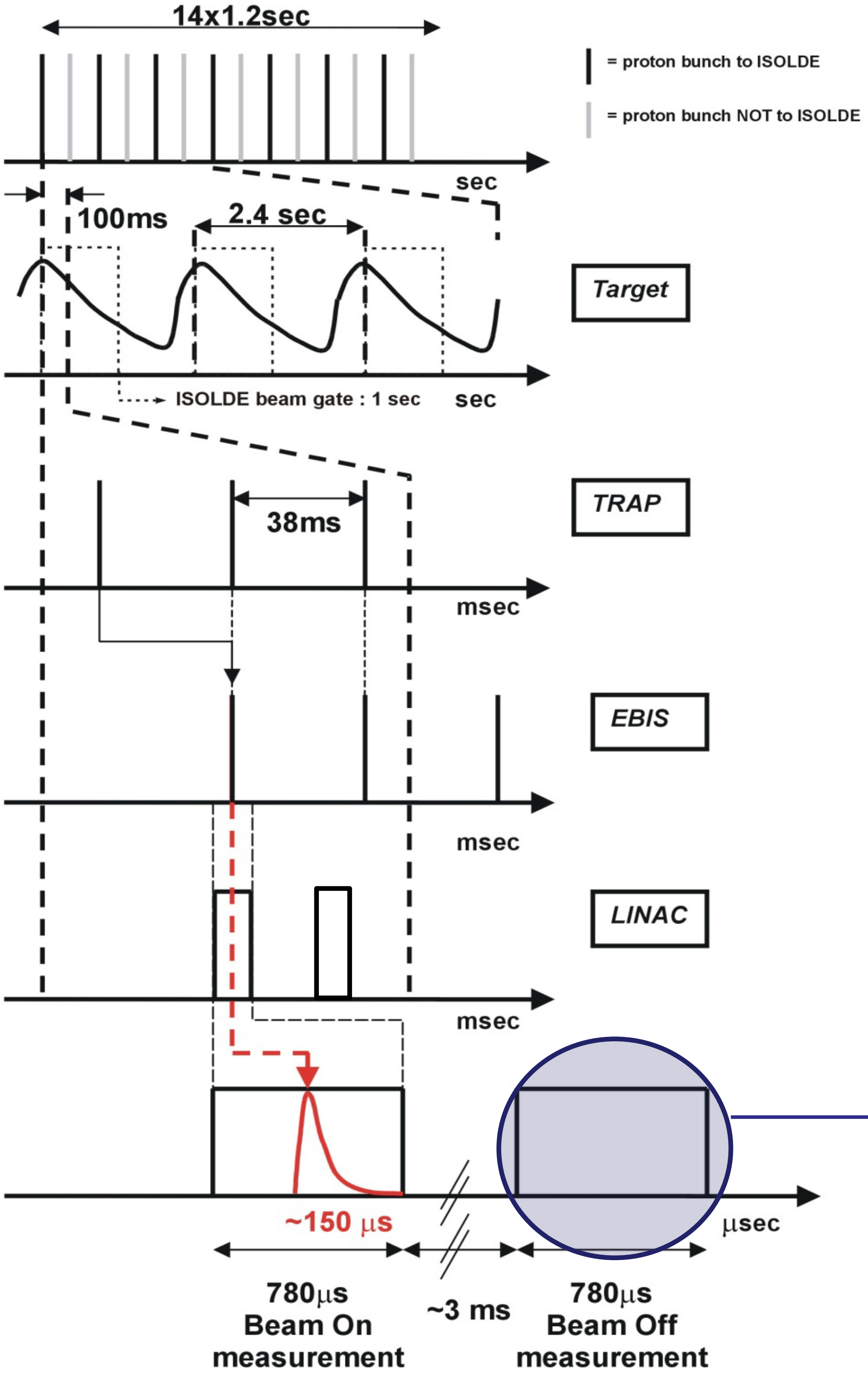

14x1.2sec
= proton bunch to ISOLDE
= proton bunch NOT to ISOLDE
sec
100ms
2.4 sec
Target
ISOLDE beam gate : 1 sec
sec
TRAP
38ms
msec
EBIS
msec
LINAC
msec
~150 μs
μsec
780μs
Beam On
measurement
~3 ms
780μs
Beam Off
measurement

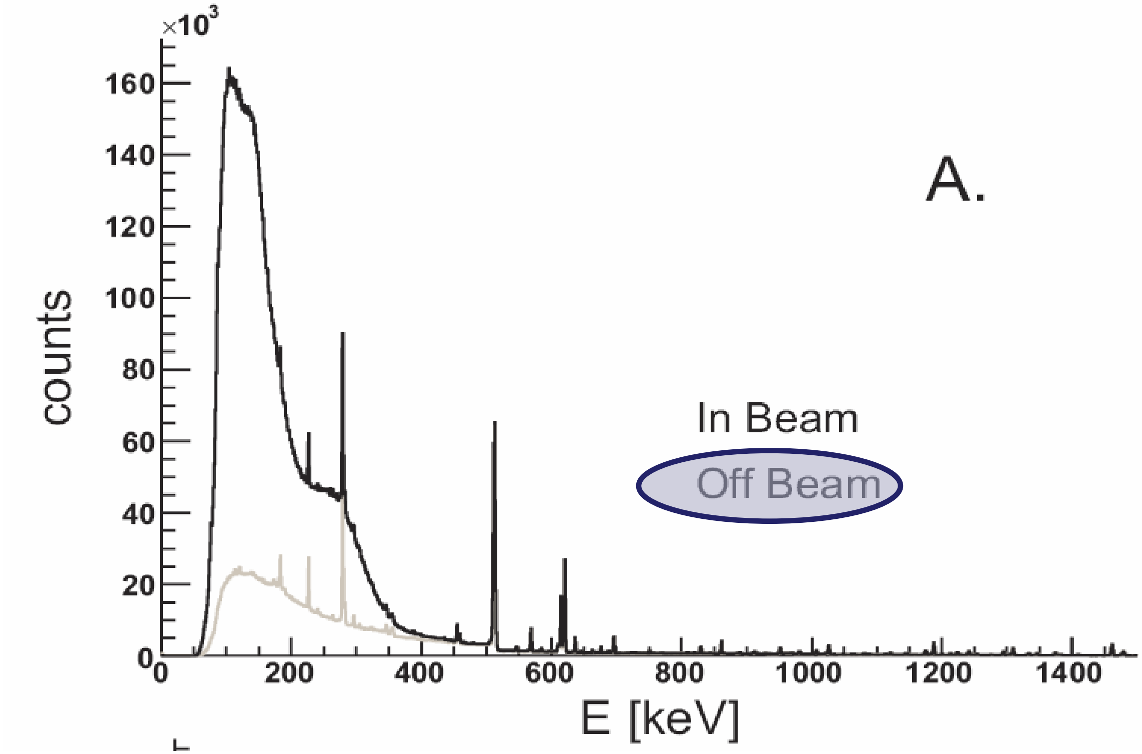

×10^3
160
140
120
100
80
60
40
20
0
counts
A.
In Beam
Off Beam
0
200
400
600
800
1000
1200
1400
E [keV]

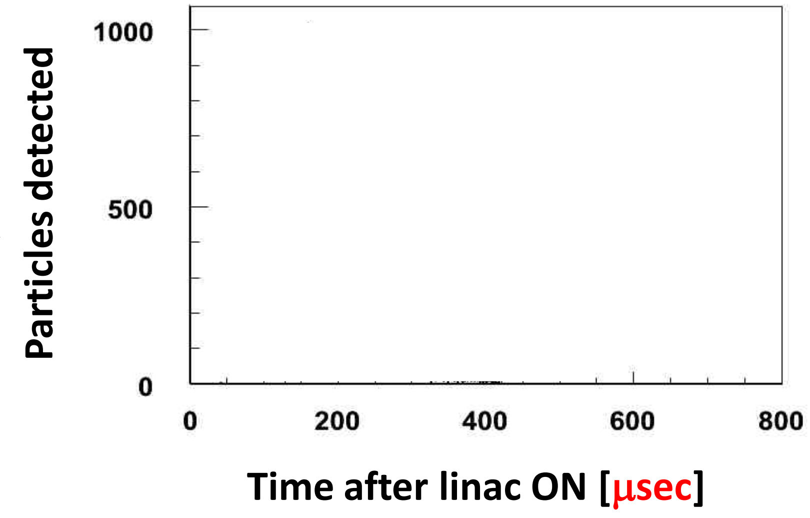

1000
500
0
Particles detected
0
200
400
600
800
Time after linac ON [μsec]

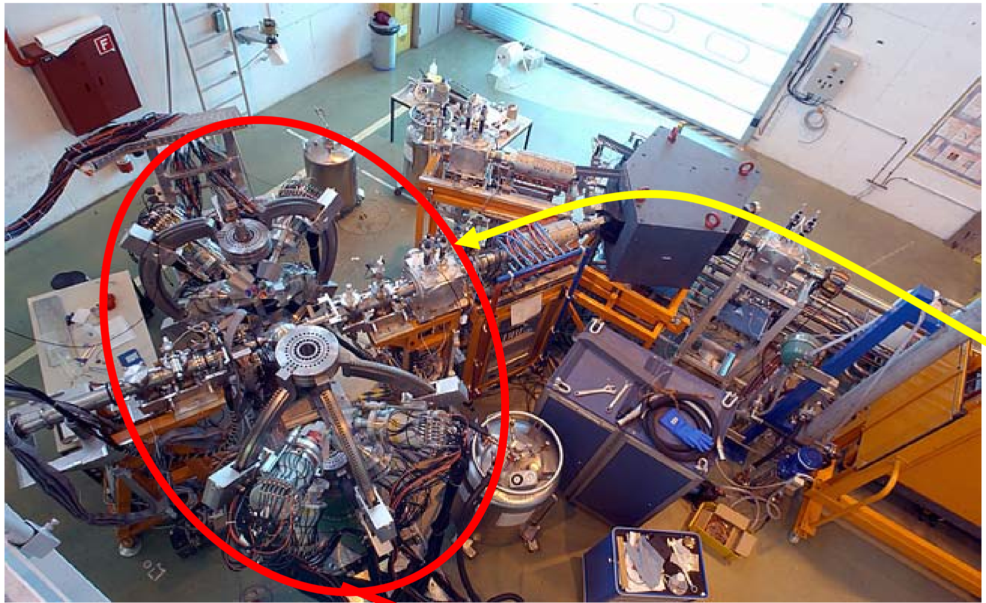

Miniball

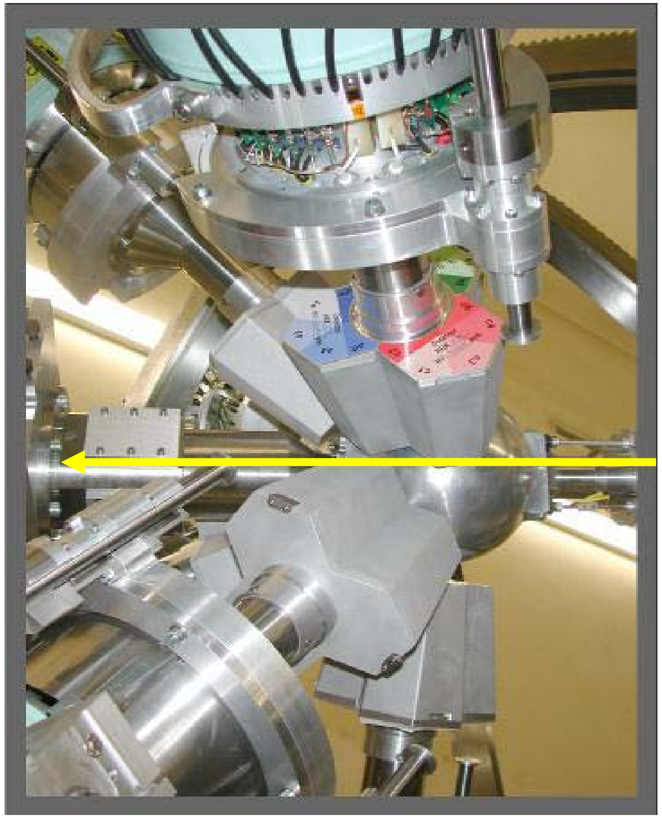

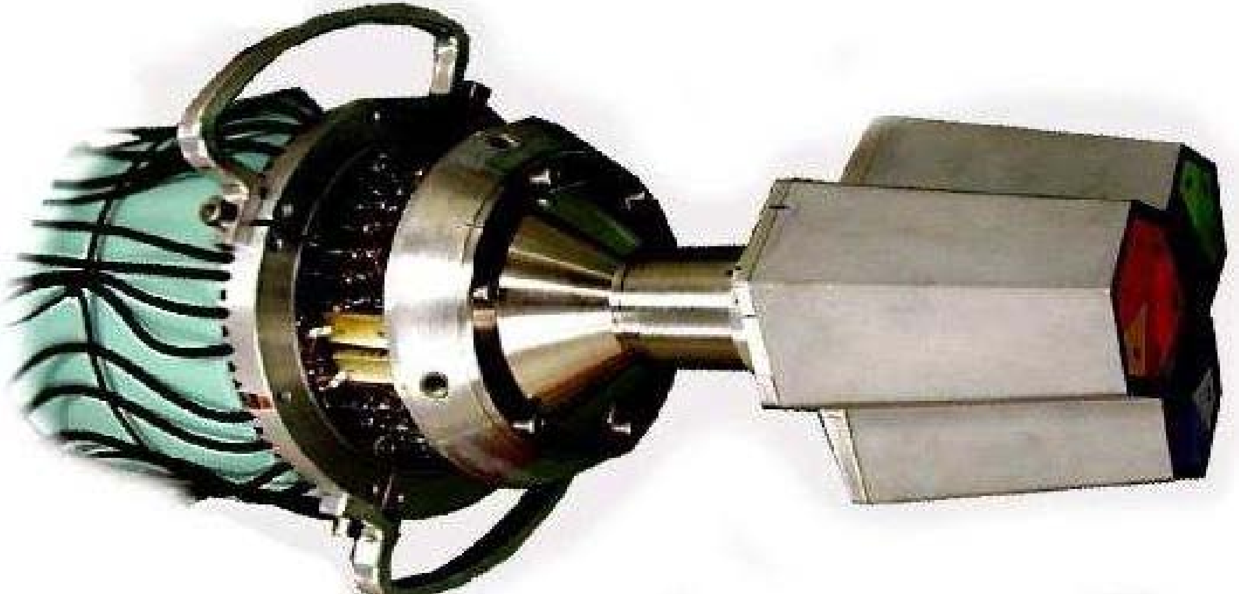

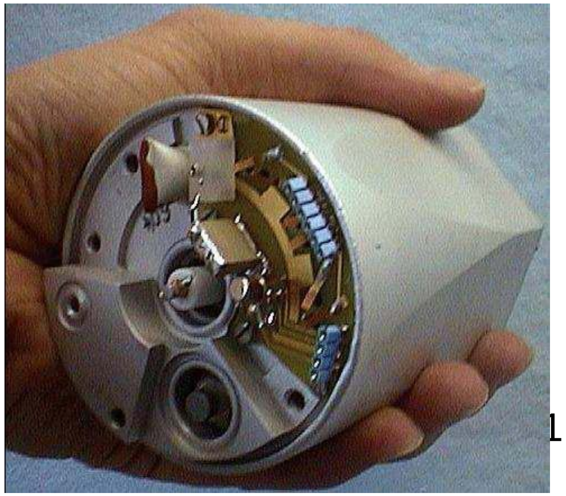

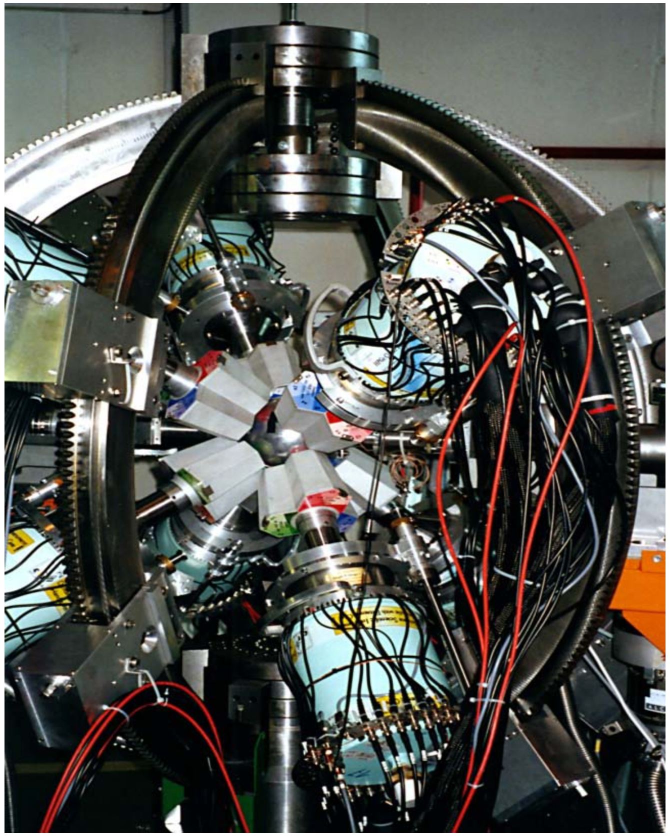

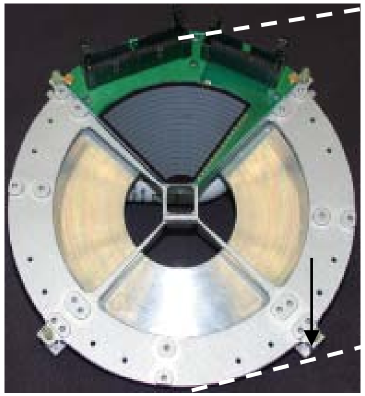

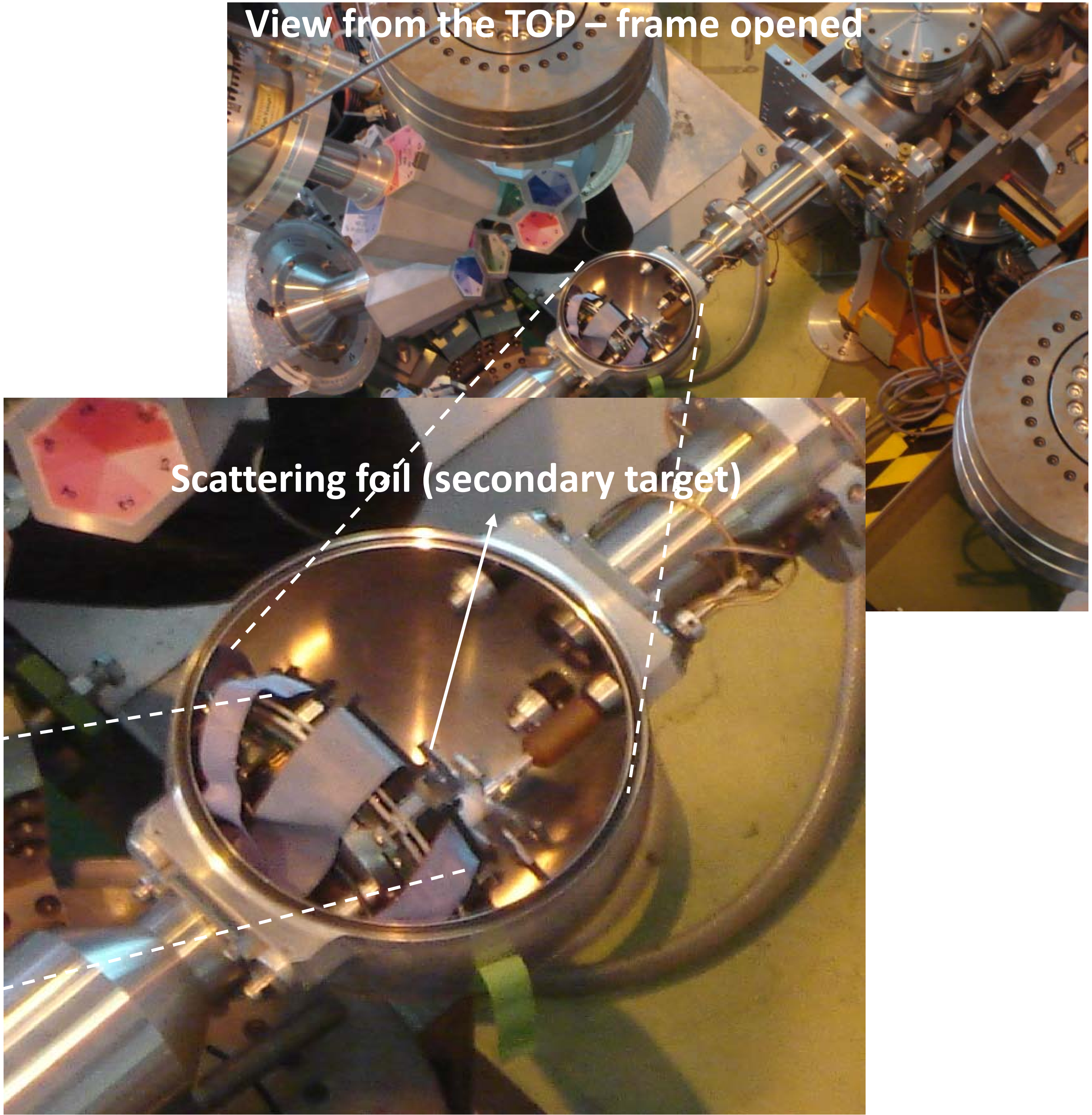
View from the TOP – frame opened
Scattering foil (secondary target)

O. Niedermaier, PRL 94 172501 (2005)

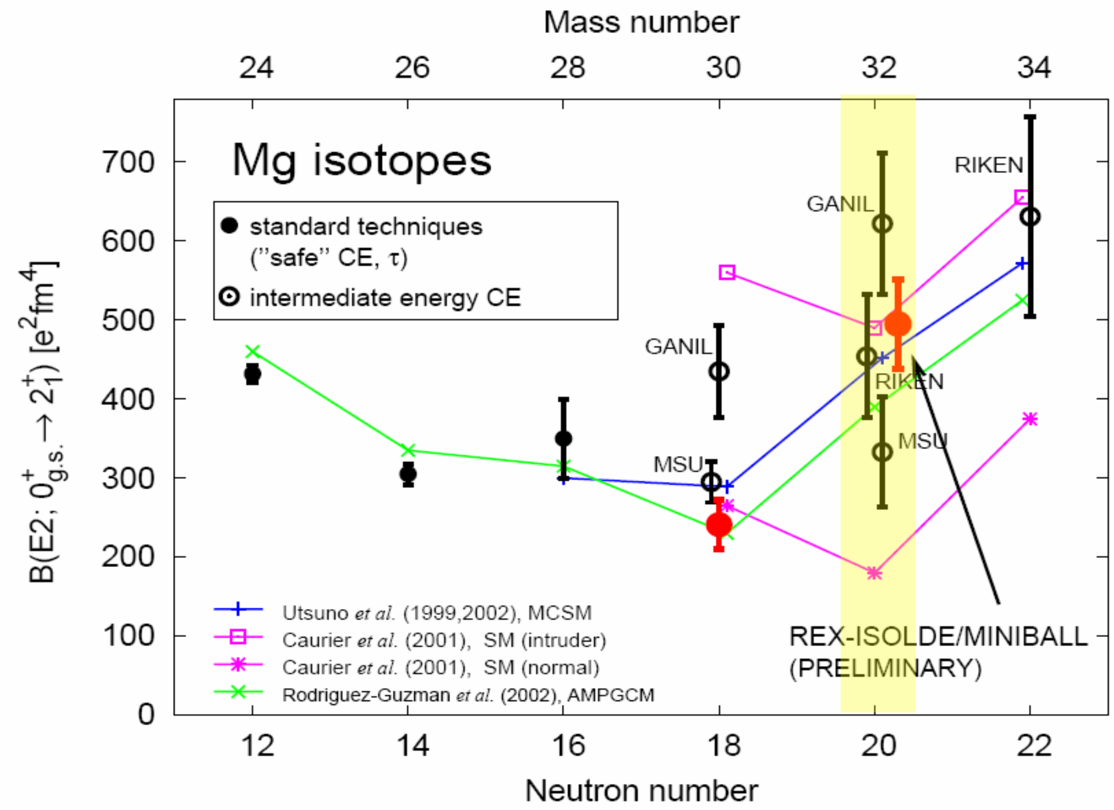

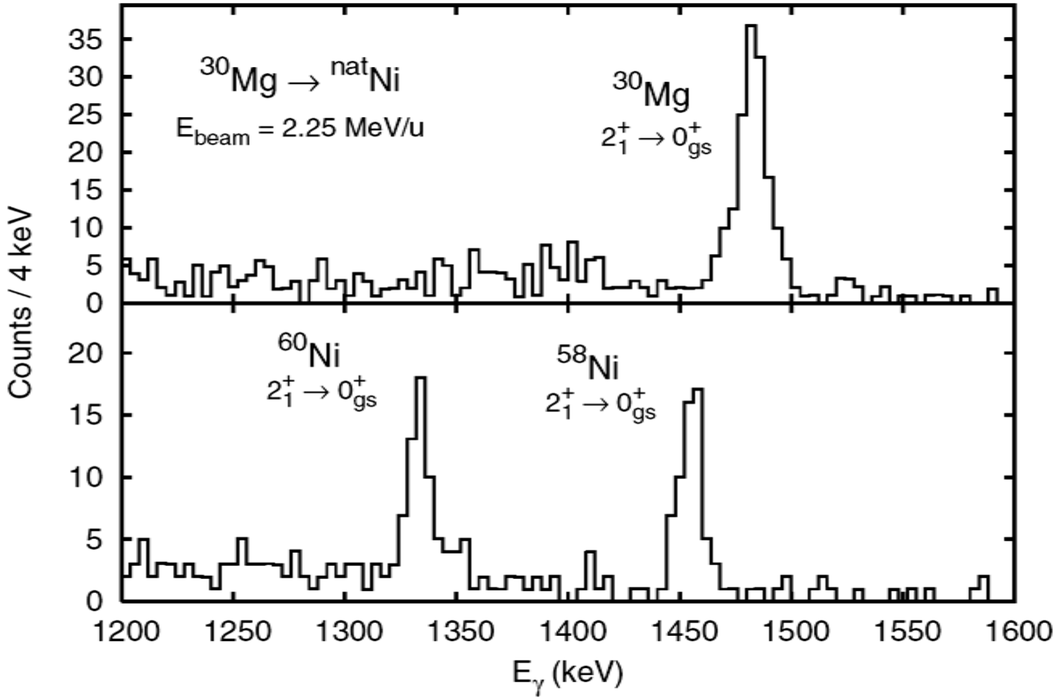

$$\frac{N_{Mg}\,(2^+ \rightarrow 0^+)}{N_{Ag}\,(3/2^- \rightarrow 1/2^-)} = \frac{I_{Mg}.\sigma_{Mg}.\varepsilon_{Mg}.\rho d.N_A}{I_{Mg}.\sigma_{Ag}.\varepsilon_{Ag}.\rho d.N_A}$$

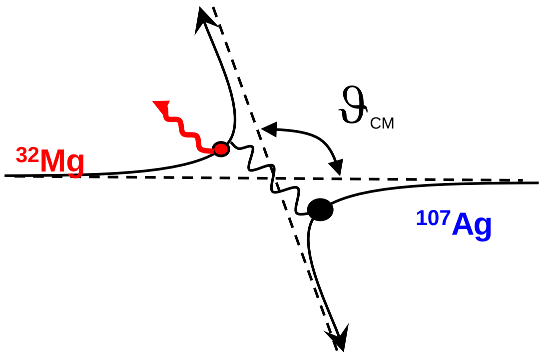

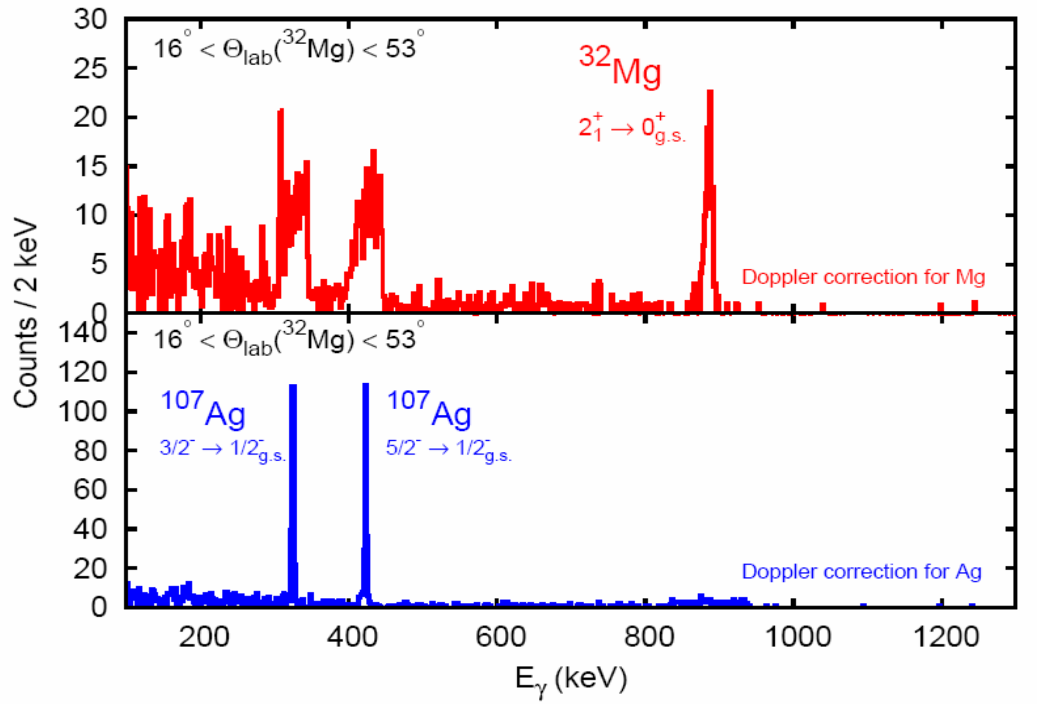

Island of Inversion: Open questions

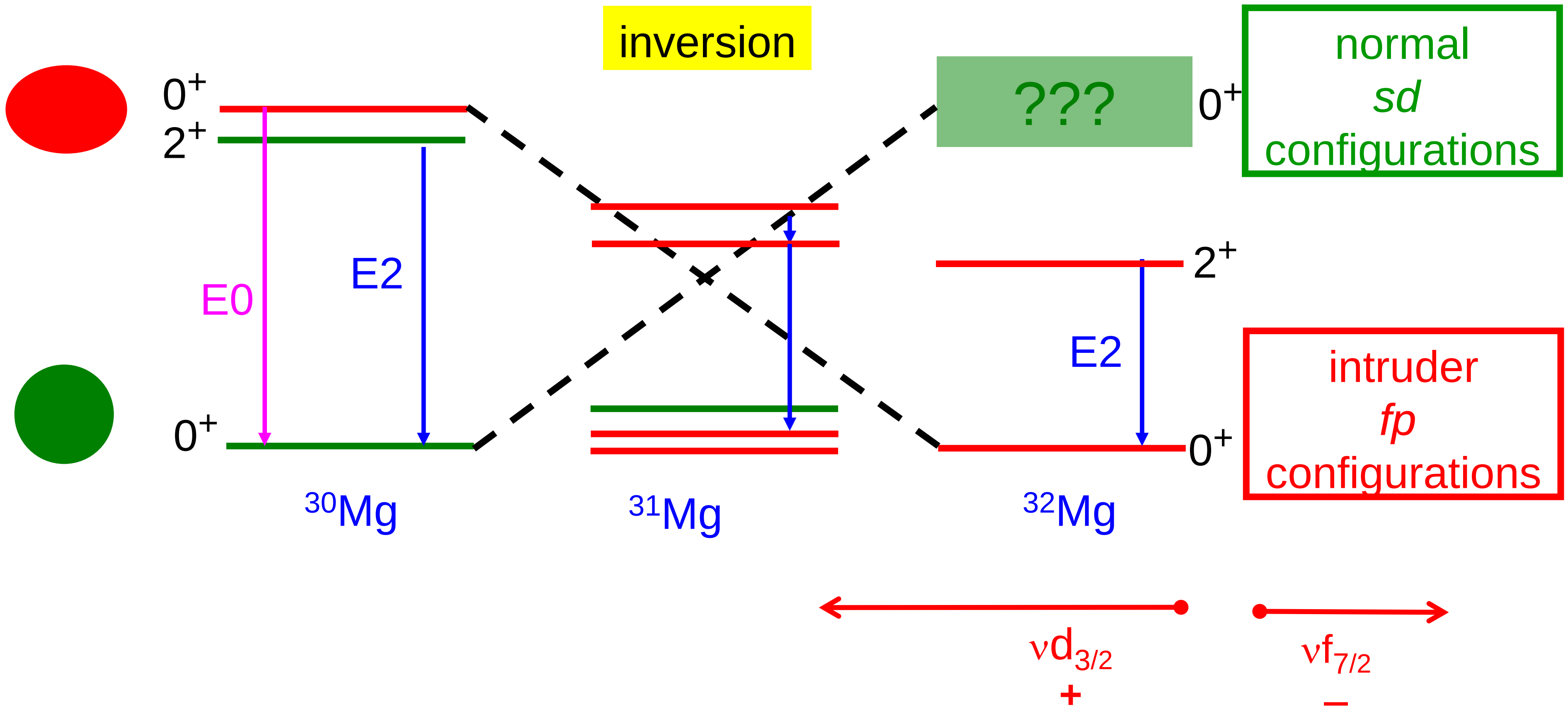

Where are the borders?

How does transition into island of inversion occur ?

Does picture of shape coexistence hold?

g-factor and spin of the ^{31,33}Mg ground state

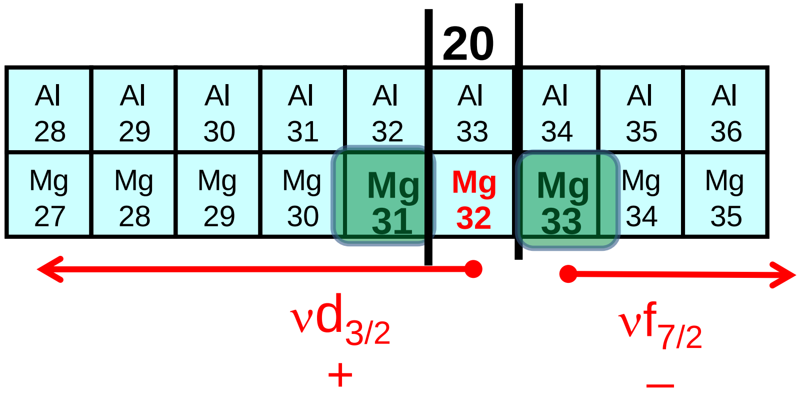

laser spectroscopy and β-NMR
g-factor and spin for ^{31}Mg and ^{33}Mg
from sign of g-factor → parity

^{31}Mg, $I^\pi = 1/2^+$ $\nu(sd)^{-3}(fp)^2$
^{33}Mg, $I^\pi = 3/2^-$ $\nu(sd)^{-2}(fp)^3$

→ pure 2p-2h intruder ground states !

Intruder ground state configurations:

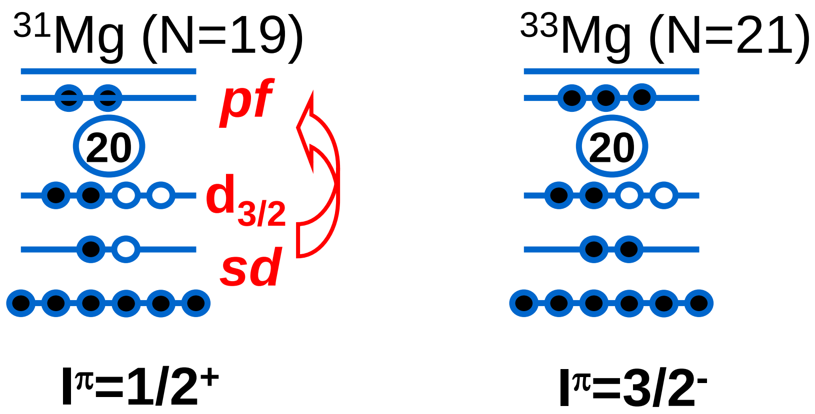

Normal ground state configurations:

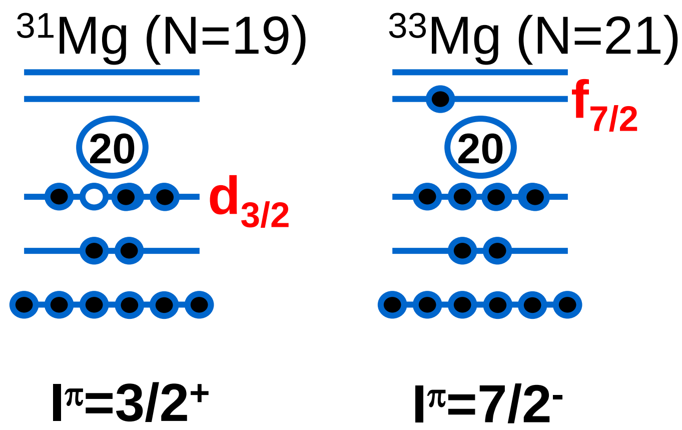

G. Neyens et al., PRL 94, 022501 (2005)
D. Yordanov et al., PRL 99, 212501 (2007)

Renewed β-decay studies

^{31}Mg F. Maréchal et al., PRC 72, 044314 (2005)
^{33}Mg V. Tripathi et al., PRL 101, 142504 (2008)

Collective properties of ^{31}Mg

– β-decay studies of ^{31}Mg at GANIL

- shell model calculation *sd-fp* valence space
  ANTOINE code, effective interaction SDPF-NR

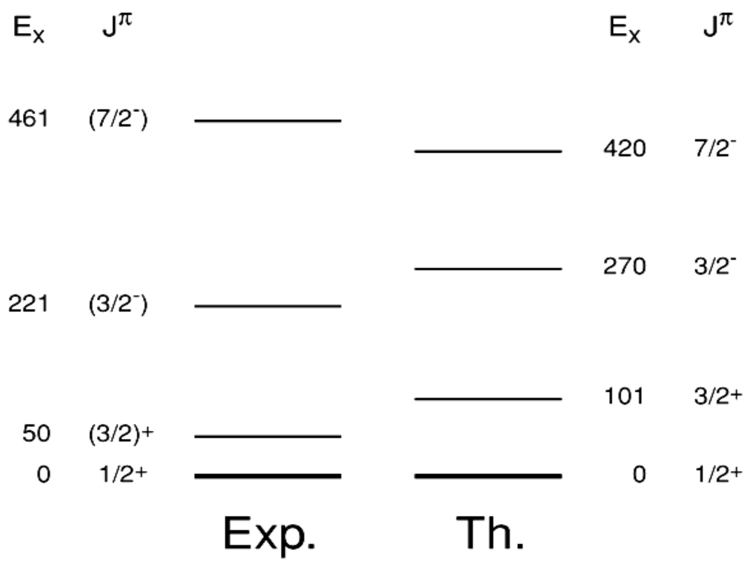

collective properties of positive K=1/2 rotational band of ^{31}Mg:
excitation energy, quadrupole moment Q, B(E2), magnetic moment μ, B(M1)

J	E_x	$n^{\nu}_{d_{5/2}}$	$n^{\nu}_{d_{3/2}}$	$n^{\nu}_{s_{1/2}}$	Q_s/Q_0	$B(E2)$	μ	$B(M1)$
1/2	0	5.62	1.99	1.33			−0.98	
3/2	101	5.63	1.77	1.56	−17/84	106	+0.56	0.06
5/2	988	5.60	2.02	1.31	−17/59	127	−0.30	0.38
7/2	1236	5.63	1.68	1.64	−25/75	151	+0.94	0.04
$K = 1/2^+$		5.75	1.52	1.73				

F. Maréchal *et al.*, Phys. Rev. C **72**, 044314 (2005)
M. Kimura, Phys. Rev. C **75**, 041302(R) (2007)

Coulomb excitation ^{31}Mg

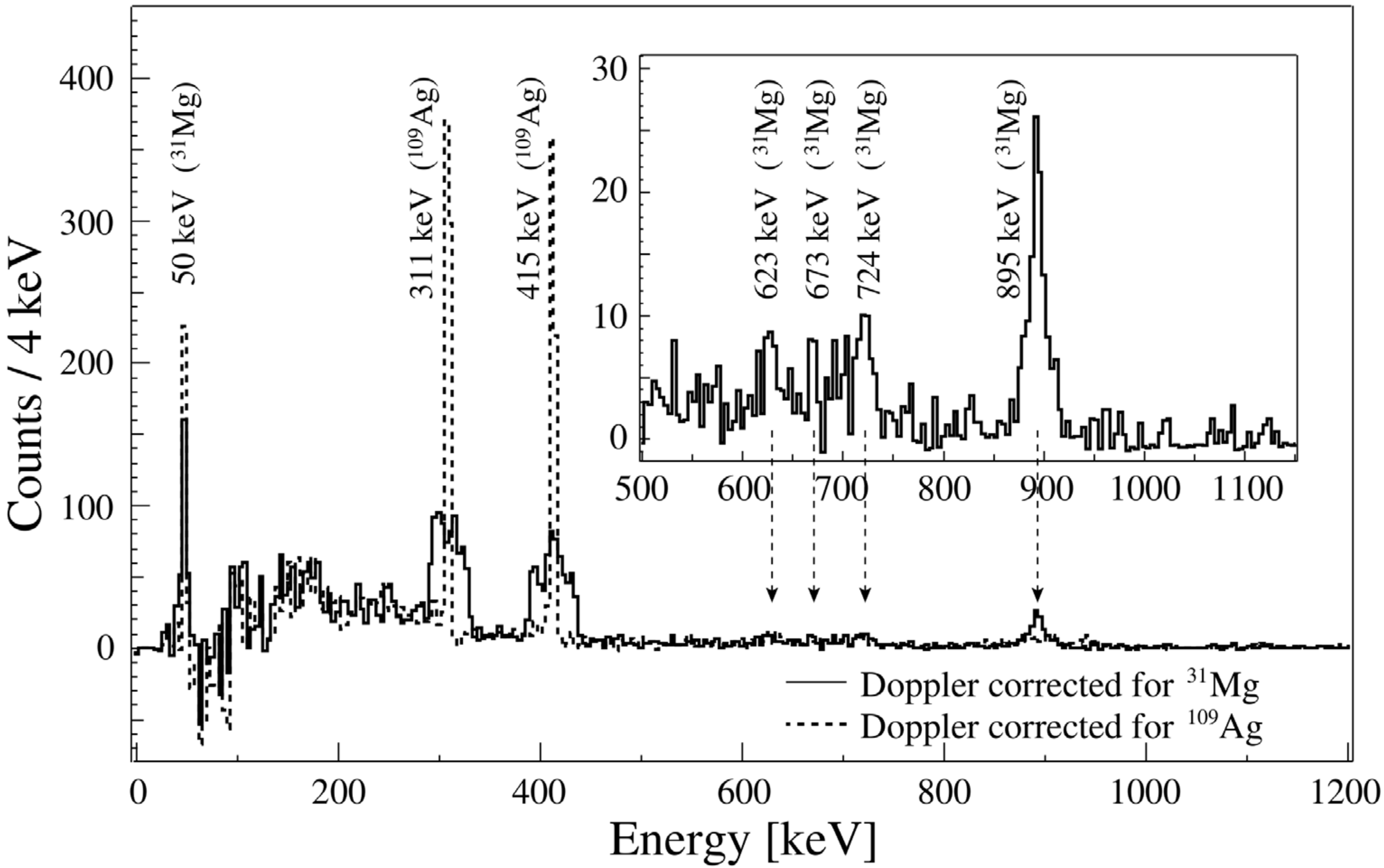

GOSIA Coulomb excitation calculation

Results:

- one step E2 excitation

$B(E2, 1/2^+ \rightarrow 5/2^+) = 182\ e^2fm^4$

- decay of (5/2+,3/2+) level via M1 transition

$B(M1, 5/2^+ \rightarrow 3/2^+) = 0.1 - 0.5\ \mu_n^2$

- results confirms strong collective excitation
- rotational sequence: $1/2^+ \rightarrow 3/2^+ \rightarrow 5/2^+$

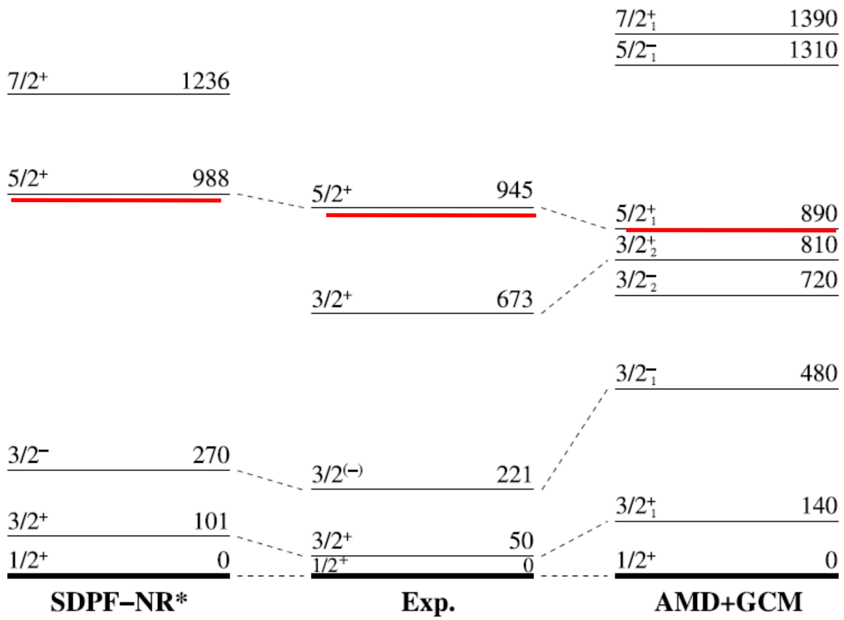

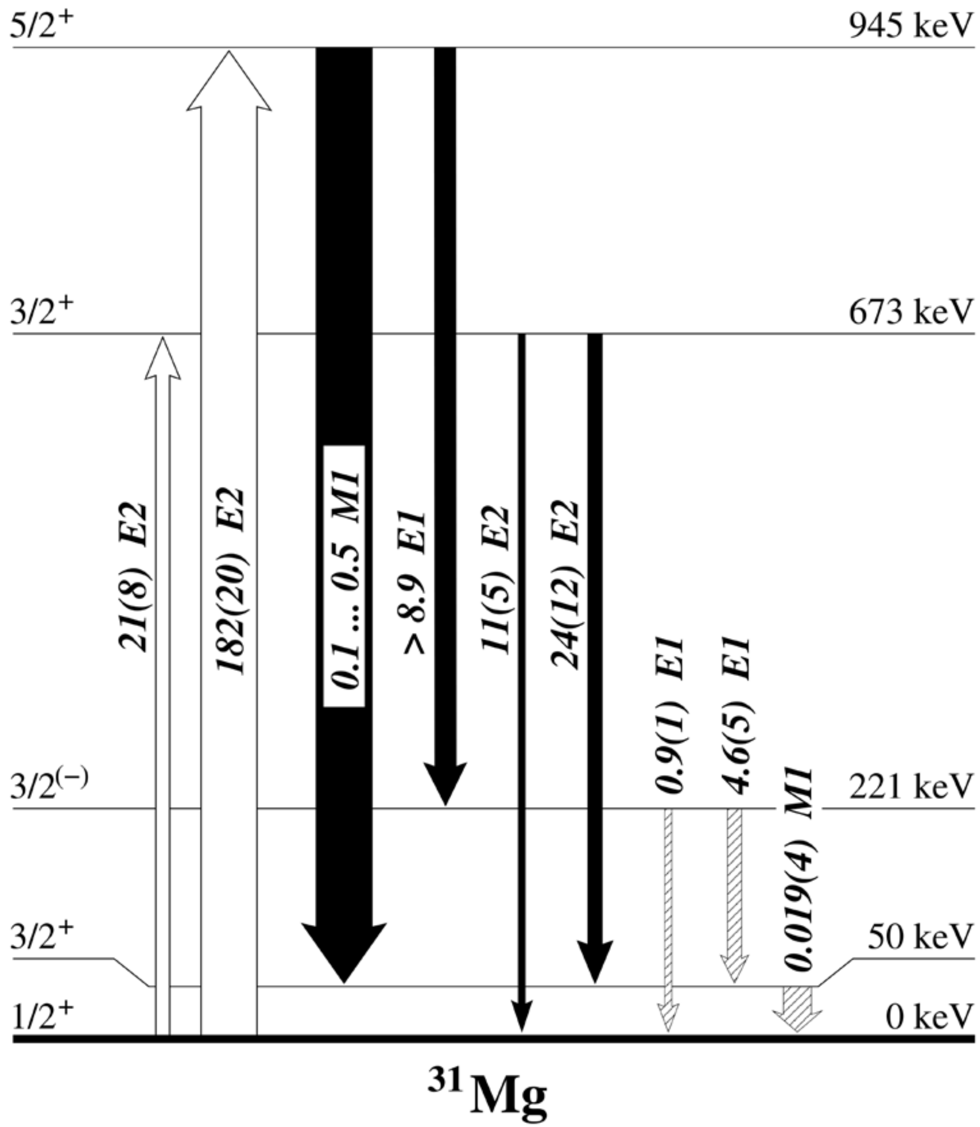

M. Seidlitz et al; PLB 700 (2011) 181

M. Kimura, Phys. Rev. C **75**, 041302(R) (2007)

Search for second 0^+ state in ^{30}Mg

Shape coexistence ?

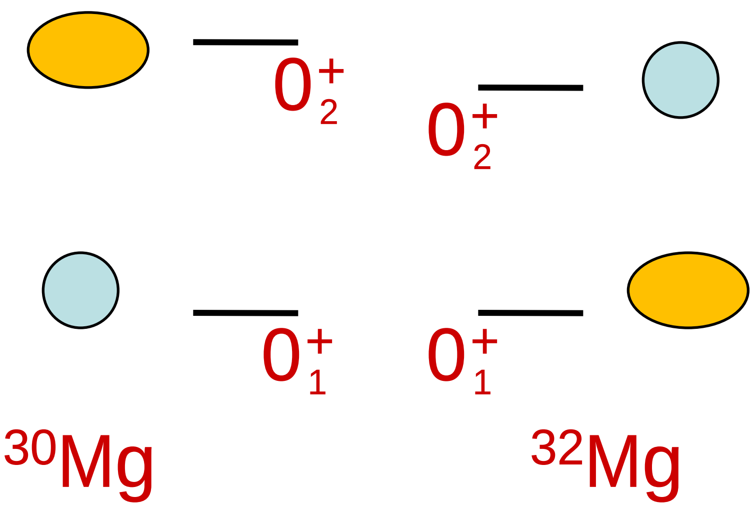

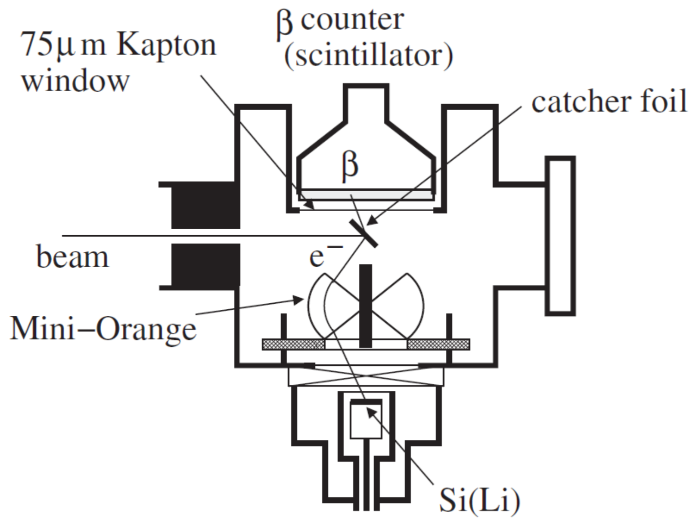

- electron spectroscopy after β-decay at ISOLDE
- first excited 0^+ state at 1789 keV in ^{30}Mg

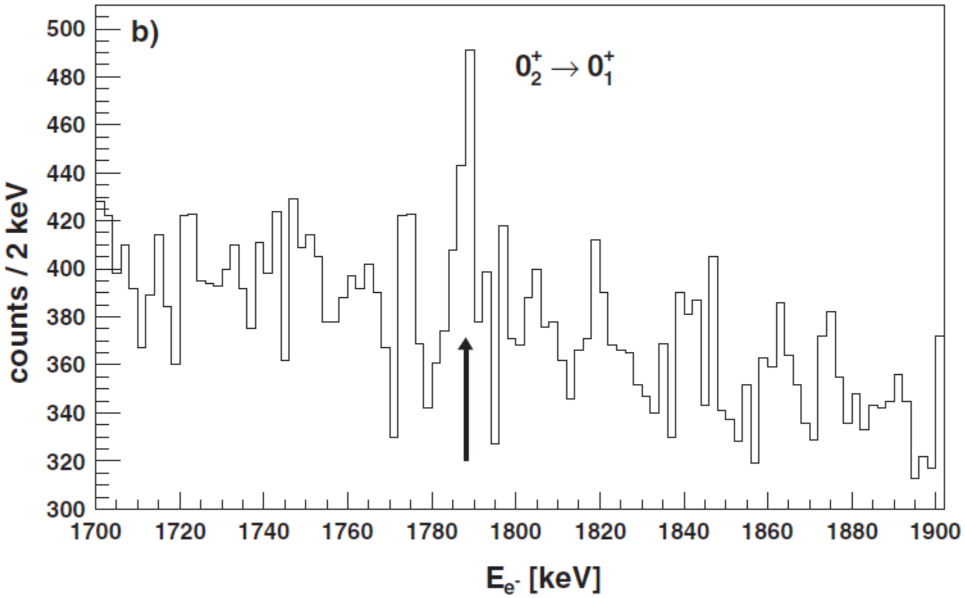

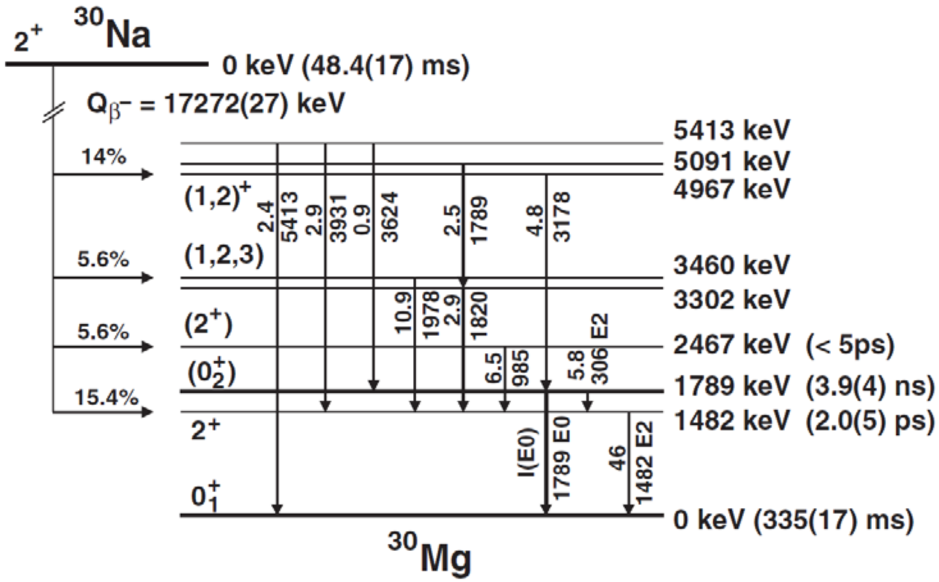

W. Schwerdtfeger, et al; PRL 103, 012501 (2009)

Shape coexistence in ^{30}Mg

electric monopole (E0) transition to ground state:
ρ^2(E0)= (26.2 (7.5)) x 10^{-3}

beyond-mean-field calculations with Gogny force:
- two competing configurations, small mixing
- largely different intrinsic quadrupole deformation
- ground state: $1d_{3/2}$ neutrons
- first excited 0^+ state: $1f_{7/2}$ neutrons

predictions for ^{32}Mg

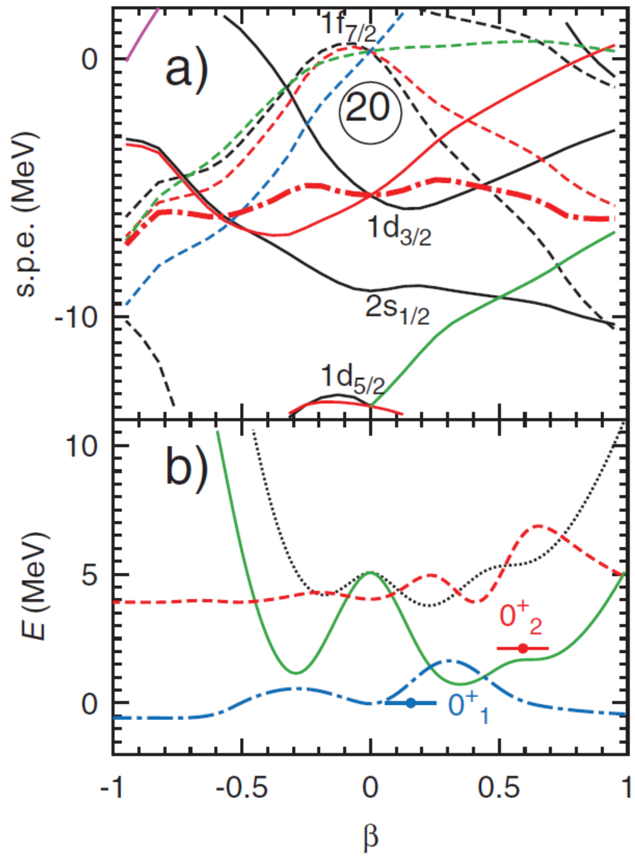

TABLE I. Results from beyond-mean-field calculations with Gogny force for ^{30}Mg and ^{32}Mg (indicated as "*T*") compared to experimental values ("*E*").

		$E_x(2_1^+)$ (MeV)	$E_x(0_2^+)$ (MeV)	$B(E2, 0_1^+ \to 2_1^+)$ (e^2 fm^4)	$\rho^2(E0) \times 10^{-3}$	$B(E2, 0_2^+ \to 2_1^+)$ (e^2 fm^4)
^{30}Mg	(*T*)	2.03	2.11	334.6	46	181.5
	(*E*)	1.482	1.789	241(31) [9]	26.2 ± 7.5	53(6)
^{32}Mg	(*T*)	1.35	2.60	455.7	41	56.48
	(*E*)	0.885	...	454(78) [5]	...	...

W. Schwerdtfeger, et al; PRL 103, 012501 (2009)

Transfer Reaction and γ-Spectroscopy

t(^{30}Mg, ^{32}Mg)p – two-neutron transfer

- ^{3}H loaded Ti foil (40 μg/cm^2 ^{3}H, 10 GBq)
- ^{30}Mg @ 2 MeV/u
- $4 \cdot 10^4$ part/s / 150 h beam on target
- Q_{00} = -295(20) keV
- Two states populated: ground state and new state at 1083(33) keV

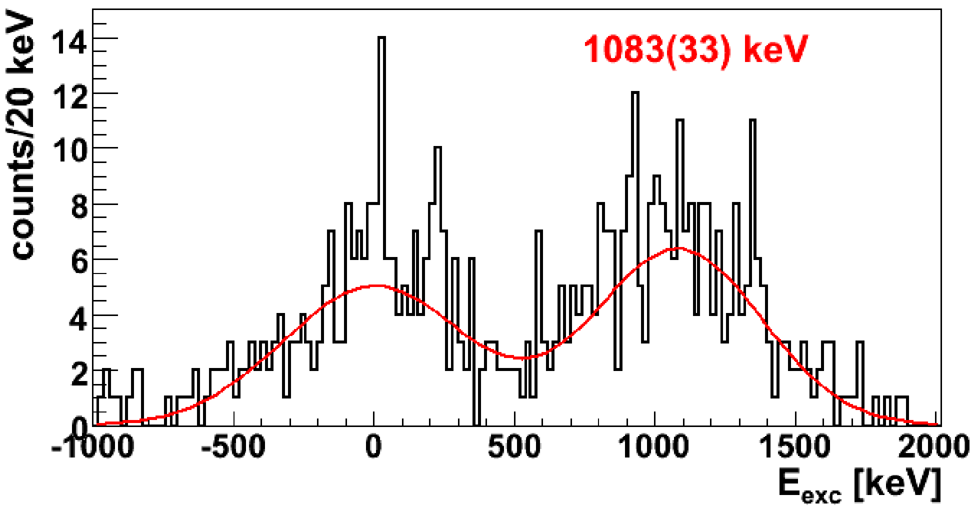

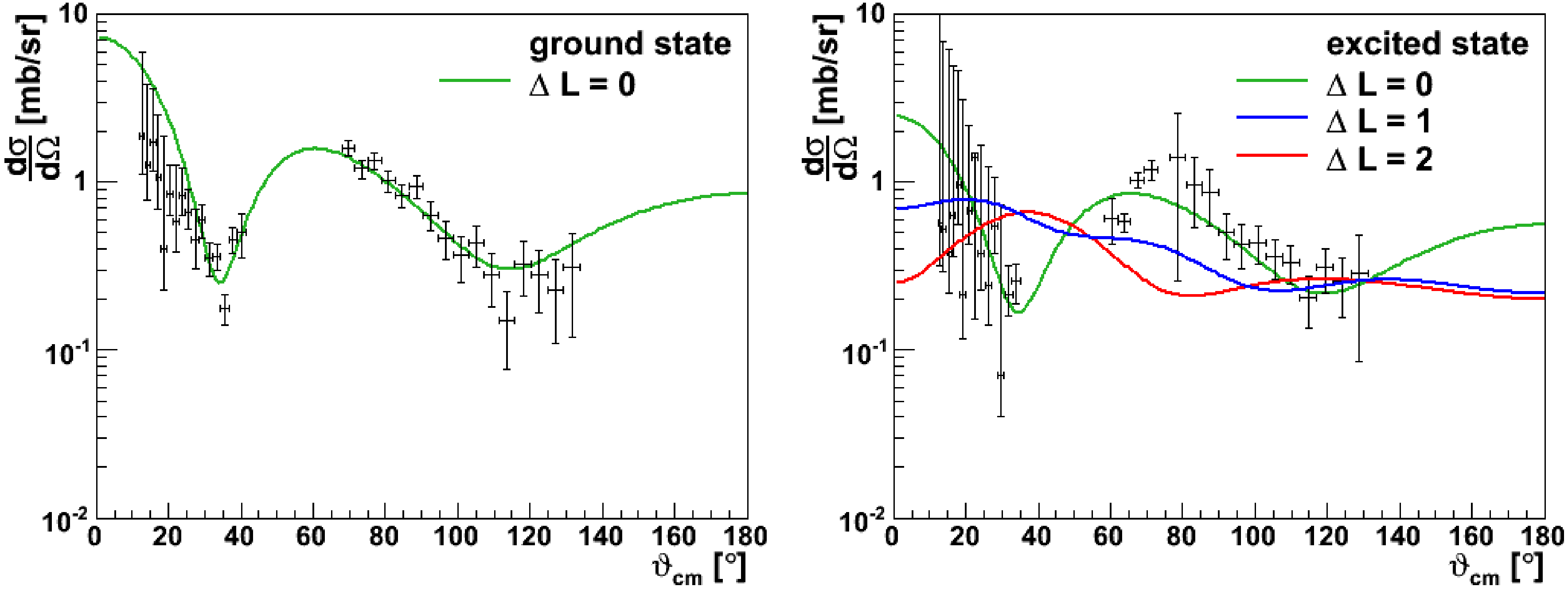

K. Wimmer et al; PRL 105, 252501 (2010)

First excited 0^+ states in ^{32}Mg

Transfer to ground state in ^{32}Mg

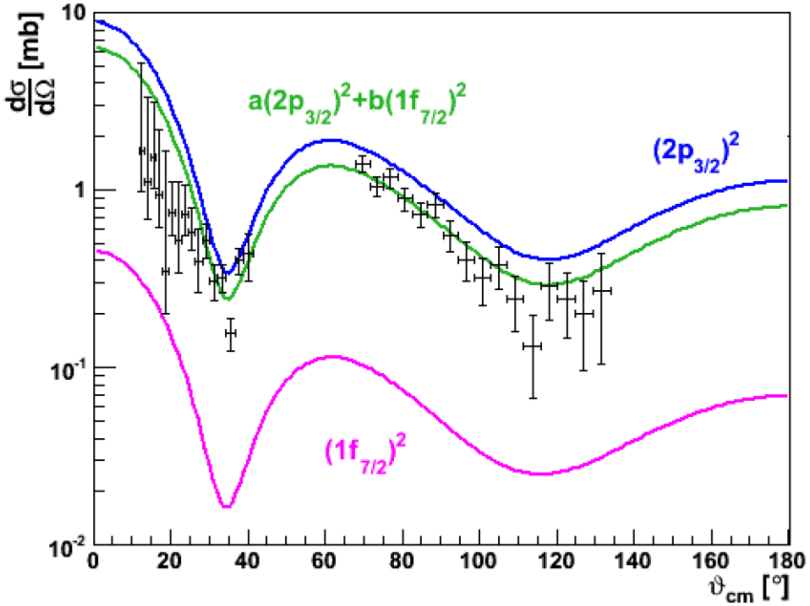

g.s. occupation numbers using effective USD / SDPF-M interactions:

B. H. Wildenthal, Prog. Part. Nucl. Phys. 1, 5 (1984) T. Otsuka et al., Prog. Part. Nucl. Phys. 47, 319 (2001)

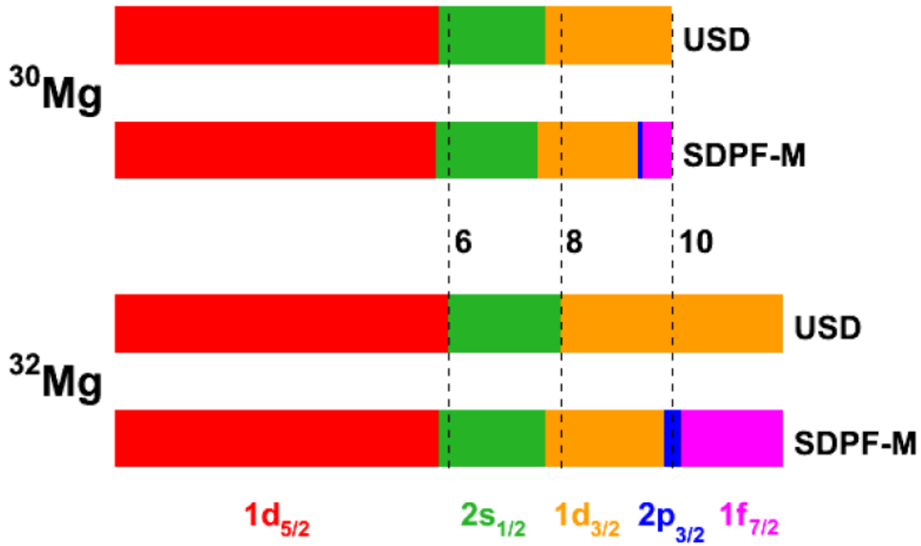

Transfer to excited 0^+ state in ^{32}Mg

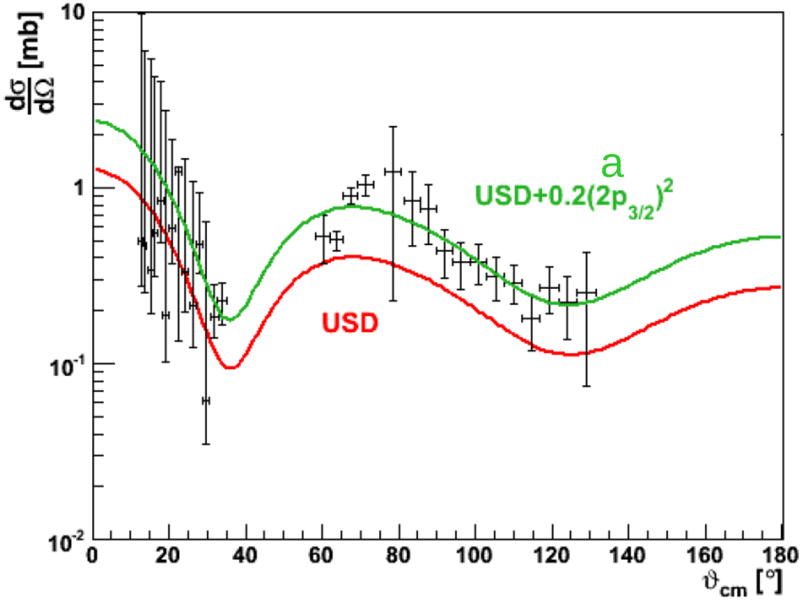

Transfer to ground state in ^{32}Mg

- pure transfer to $(f_{7/2})^2$ to small
- large contribution from $(p_{3/2})^2$ needed (a > 0.7)

… SDPF-M underestimates the $\nu p_{3/2}$ content in the wave functions

Transfer to excited 0^+ state in ^{32}Mg

- wave function similar to g.s. in ^{30}Mg
- two-neutron spectroscopic amplitudes for pure sd → sd transitions
- cross section underestimated, small $(p_{3/2})^2$ amplitude ($a \approx 0.3$)

K. Wimmer et al; PRL 105, 252501 (2010)

Summary:Island of inversion

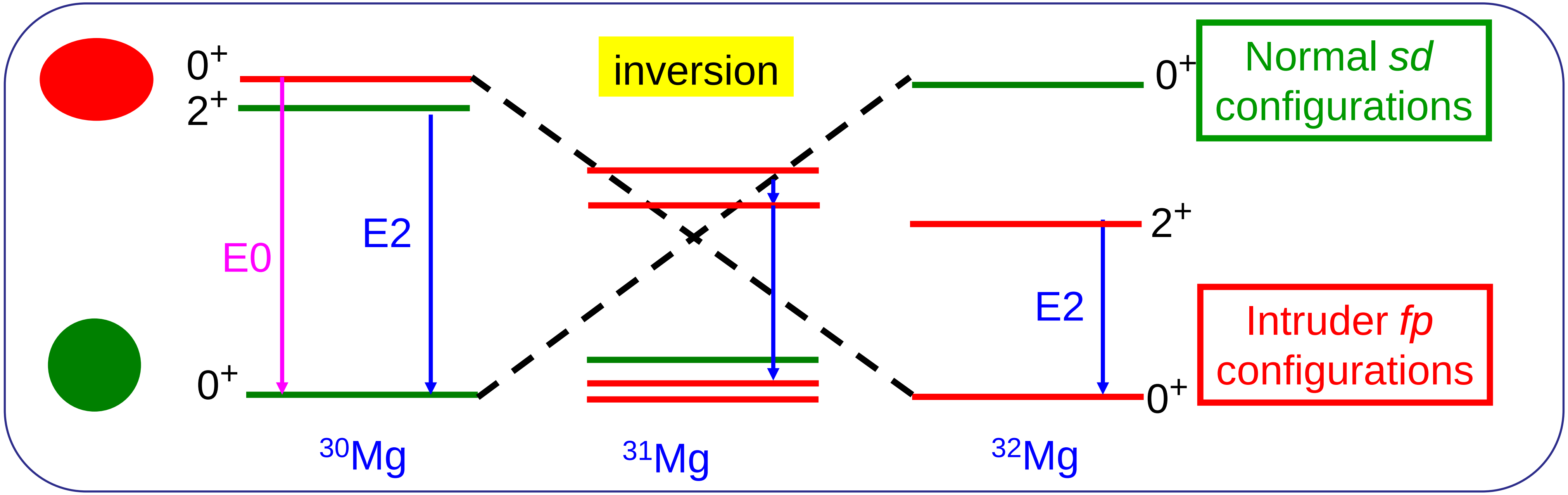

Summary:Island of inversion